



**THE EFFECT OF BOBBIN FRICTION STIR WELDING
REPETITION PROCESS ON THE MICROSTRUCTURE OF THE
ALUMINIUM ALLOY 1100**

This report submitted in accordance with requirement of the University Teknikal
Malaysia Melaka (UTeM) for Bachelor Degree of Manufacturing Engineering



YUWENDRAN A/L VELLASAMY

B051620006

960603-08-5209

FACULTY OF MANUFACTURING ENGINEERING

2019

DECLARATION

I hereby, declared this report entitled “The Effect of Bobbin Friction Stir Welding Repetition Process on the Microstructure of the Aluminium Alloy 1100” is the result of my own research except as cited in references.

Signature :

Author's Name : YUWENDRAN A/L VELLASAMY

Date : 27/12/2019



APPROVAL

This report is submitted to the Faculty of Manufacturing Engineering of Universiti Teknikal Malaysia Melaka as a partial fulfilment of the requirement for Degree of Manufacturing Engineering (Hons). The member of the supervisory committee are as follow:



ABSTRAK

Bahan yang digunakan sebagai bahan kerja untuk disertai dalam kajian ini adalah aloi aluminium 1100. Alloy aluminium 1XXX adalah bentuk aluminium yang murni kerana ia mengandungi minimum 99.00% aluminium. Kimpalan pengadukan Bobbin (BSFW) serasi untuk kimpalan AA 1100 kerana ia merupakan proses mesra alam yang mengurangkan pengeluaran haba dan pencemaran. Masalah bagi kajian ini adalah untuk memahami pengubahsuaian ciri-ciri bahan apabila kaedah multipass digunakan. Selain itu, cabaran lain adalah untuk menentukan kemampuan multipass untuk membaiki sendi dengan menggabungkan semula. Di samping itu, sambungan antara harta mekanikal sifat bahan dan logam perlu dipastikan untuk menganalisis keupayaan multipass untuk menghasilkan sambungan kimpalan yang baik. Kaedah untuk menyelesaikan masalah adalah dengan menjalankan percubaan untuk mengenal pasti peningkatan ciri-ciri bahan oleh multipass dan menemui di mana jumlah pas akan menghasilkan bersama dengan kualiti yang tinggi. Kaedah yang sama akan berguna untuk menentukan sama ada multipass boleh membantu menyambung semula kimpalan untuk dihasilkan bersama. Tambahan lagi, kaedah metalurgi dilakukan untuk mengkaji sifat sampel logam. Kaedah metallurgical yang digunakan untuk kajian ini adalah mikroskop optik (OM) dan mikroskop elektron pengimbasan (SEM) untuk memerhatikan evolusi struktur mikro dan juga perisian yang dikenali sebagai ImageJ digunakan untuk menentukan saiz butiran. Mesin mikrohardness digunakan untuk menganalisis kekerasan sampel dan ujian kekuatan tegangan muktamad juga dijalankan. Setelah melakukan kajian, hasil yang dijangkakan adalah penentuan bilangan pas yang dapat meningkatkan sifat material dan juga untuk memperbaiki sendi. Kemudian, korelasi antara harta mekanik dan harta logam boleh dibuat berdasarkan kajian yang dijalankan. Oleh itu, dengan menggunakan proses (BSFW) yang memperkenalkan haba yang rendah akan menjadikannya sebagai proses kimpalan keadaan pepejal yang sesuai untuk AA 1100.

ABSTRACT

The material used as a work piece to be joined in this study is Aluminium alloy 1100. Aluminium alloy 1XXX is a pure form of aluminium as it contains minimum 99.00 % of aluminium. Bobbin friction stir welding (BSFW) is compatible for welding AA 1100 as it is an environmental friendly process that reduce the production of heat and pollution. The problem for this study is to understand the modification in characteristic of material when multipass method utilized. Moreover, another challenge is for determining the capability of multipass for repairing joint by rejoin. In addition, connection between mechanical property of a material and metallurgical properties need to be determined for analyzing the ability of multipass for producing good weld joint. Methods for solving the problem is by conducting the experiment to identify improvement of in characteristic of material by multipass and discover at which number of passes will produce joint with high quality. The same method will be useful for determining whether multipass can help for rejoining of weld for the joint produced. Furthermore, metallurgical method done for examining metallurgical property of sample. Metallurgical method used for the study is optical microscope (OM) and scanning electron microscope (SEM) for observing the microstructure evolution and also software known as ImageJ used for determining the grain size. Microhardness machine utilized for analyzing the hardness of sample and ultimate tensile strength test also carried out. After performing the study, expected outcome is determination of which number of passes can improve material characteristic and also for repairing the joint. Then, correlation between mechanical property and metallurgical property can be made based on the study carried out. Thus, by using (BSFW) process that introduce low heat will make it as a suitable solid-state welding process for AA 1100.

DEDICATION

TO MY DEAREST PARENTS,

Mr Vellasamy Subbiah and Mrs. Komalavalli Ramasamy

TO MY BELOVED SISTER,

Sobitha Vellasamy

TO MY HONOURED SUPERVISOR

Dr. Mohammad Kamil Bin Sued

*For his advices, support, motivation and guidance during
accomplishment of this project*

UNIVERSITI TEKNIKAL MALAYSIA MELAKA

TO ALL STAFF & TECHNICIANS

For their direction and advices during completion of this project

TO MY MOTIVATOR

Keerthisha Vasudevan

For your love, motivation and support

TO MY SUPPORTIVE FRIENDS

ACKNOWLEDGMENT

I would like to convey my sincere gratitude to my honored supervisor, Dr Mohammad Kamil bin Sued, for his great mentoring, guidance and his kindness given to me to accomplish my project. His supervision and valuable advice helped by exposing me to the vital problems involved and its solution regarding the project title and accomplishment of my Final Year Project on time as per fulfilling the requirements for my Bachelor's Degree.

I want to say my special thanks to Dr, Zurina binti Shamsudin for her guidance throughout this project, especially in writing report and also for preparing presentation poster according to the required format aspect.

Furthermore, I want to extend my thanks all my friends, undergraduate teammates, all technicians, and every single person for giving me a lot of motivation, guidance and moral support in completing this project.

UNIVERSITI TEKNIKAL MALAYSIA MELAKA

TABLE OF CONTENT

Abstrak	i
Abstract	ii
Dedication	iii
Acknowledgement	iv
Table of Contents	v
List of Tables	vii
List of Figures	viii
List of Abbreviations	xi
List of Symbols	xiii
CHAPTER 1: INTRODUCTION	
1.1 BACKGROUND STUDY	1
1.2 PROBLEM STATEMENT	4
1.3 OBJECTIVE	5
1.4 SCOPE OF RESERCH	6
1.5 SIGNIFICANT OF STUDY	7
CHAPTER 2: LITERATURE REVIEW	
2.1 DEFECT IN FRICTION STIR WELDING (FSW)	8
2.1.1 REPAIR PROCESS IN WELDING	12
2.1.2 REPETITION METHOD IN FUSION WELDING	12
2.1.3 MULTIPASS FOR SOLID STATE JOINING	16
2.2 IMPACT OF PROCESS PARAMETER	18
2.2.1 TEMPERATURE	19

2.2.2	MECHANICAL ANALYSIS	20
2.2.3	MICROSTRUCTURE ANALYSIS	22
2.3	MATERIAL BEHAVIOUR IN REPAIRING	25
2.3.1	HEAT FROM MULTIPASS	26
2.3.2	PRESENCE OF CONTAMINATION	28
2.3.3	ADDITIONAL MATERIAL / FILLER	30
2.4	MICROSTRUCTURE EVOLUTION IN WELDING	33
2.4.1	EFFECT OF PROCESS PARAMETER	33
2.4.2	FOR REPAIRING	37
2.5	CURRENT WORK IN (FSW) MULTIPASS	43
2.6	METALLURGICAL WORK FOR GRAIN STRUCTURE	52
2.7	CONCLUSION	53
CHAPTER 3: METHODOLOGY		
3.0	INTRODUCTION	55
3.1	FLOWCHART OF PROCESS	56
3.2	PARAMETER SETUP FOR MULTIPASS BFSW	57
3.2.1	PREPARATION OF WORKPIECE FOR EXPERIMENT	57
3.2.2	TYPE OF BOBBIN TOOL USED	58
3.2.3	EXPERIMENT SETUP	58
3.2.4	SETUP FOR BFSW WELDING	59
3.3	SAMPLE PREPARATION	59
3.4	MICROHARDNESS TESTING	60
3.5	OPTICAL MICROSCOPE	61
3.6	SCANNING ELECTRON MICROSCOPE	62
3.7	GRAIN SIZE MEASUREMENT	63
3.8	ANALYSIS FOR POROSITY LEVEL IN SAMPLE	66
3.9	ULTIMATE TENSILE TESTING	67

CHAPTER 4 : RESULT & DISCUSSION	
4.1 VISUAL INSPECTION OF WELDED JOINT	68
4.2 MICROSTRUCTURAL OBSERVATION UNDER OPTICAL MICROCOPE	69
4.3 HARDNESS TEST RESULT	72
4.4 ANALYSIS OF ULTIMATE TENSILE TESTING	83
4.5 MICROSTRUCTURAL OBSERVATION UNDER SCANNING ELECTRON MICROCOPE	85
4.6 RESULT FROM FLUID SATURATION LEVEL TEST	86
CHAPTER 5 : CONCLUSION AND RECOMMENDATION	87
5.1 SUSTAINABILITY	88
5.2 RECOMMENDATION	89
REFERENCE	90
APPENDIX	96



LIST OF TABLES

2.1	Parameter of welding for (SMAW)	14
2.2	Parameter of welding for (GMAW)	14
2.3	Set up of parameter used during (FSW) process	17
2.4	Parameter for FSW welding of AA6063 and A319	22
2.5	Direct impact of process parameter	23
2.6	Parameter set up for this investigation	24
2.7	Parameter used for welding	35
2.8	Previous works regarding multipass	54
2.9	Parameter setup for the experiment	58
3.1	Steps to calculate average grain size	64
3.2	Steps that need to be performed for fluid saturation level test	66
3.3	Machine specification of tensile testing machine	67
4.1	OM image at weld zone area with average grain size for a) one pass (3.87 μm), b) two pass (2.54 μm) and c) three pass (3.22 μm) at magnification of 10X	70
4.2	Indentation at each zone for One Pass	73
4.3	Indentation at each zone for Two Pass	76
4.4	Indentation at each zone for Three Pass	79
4.5	Result of ultimate tensile testing for samples	83
4.6	SEM image at weld zone area for A) one pass, B) two pass and C) three pass magnification of 1000X.	85
4.7	Results from fluid saturation level test	86

LIST OF FIGURES

1.1	Types of FSW. (a) CFSW (b) BFSW	2
2.1	Schematic drawing of (FSW) process	8
2.2	Scanning electron microscope image of kissing bond defect	9
2.3	Joint line remnant in (FSW) by macrograph	10
2.4	Tunneling defect	11
2.5	Schematic drawing of thirteen passes of 316L stainless steel filler rod	13
2.6	Weld passes of profile for (a) original welding, (b) partial repair weld and (c) full repair welding	15
2.7	Hardness maps of cross-sectional area for: (a) two- and (b) one-pass welded joints	18
2.8	Difference of emissivity with temperature	20
2.9	Zones formed in FSW joint performed	25
2.10	Macro and microstructures in (FSW) joints by using conical stirrer pin	25
2.11	Macro and microstructures in (FSW) joints by using the triangular stirrer pin	26
2.12	Schematic diagram of multipass (FSW) process done	27
2.13	Image for transverse cross-section of the weld (a) and enlargement image of the Al-Fe interface (b to e)	28
2.14	Schematic diagram of making CNT/2009Al composite sequence	29
2.15	Image of TEM for CNT-AL alliance	30
2.16	Schematic diagram for D-FFSR process: (a) volume defects, (b) stage of drilling, (c) include fillers, (d) stage of filling and (e) stage for retracting	31
2.17	Cross section of repaired joint	32
2.18	Material behaviour at filling stage	33
2.19	Surface of joint and its macrostructure at variation of speed	35
2.20	The impact of tool traverse speed on the tensile strength for the welded joint	36
2.21	Microstructure of joint welded at 200 mm/min	37
2.22	Schematic drawing of (FSP) process	38
2.23	Macrostructure of Al-Si alloy that underwent to the (FSP) process	39

2.24	Microstructure of stir zone for (a) FSW welded joint and (b) FSP for AlSi9Mg	40
2.25	Microstructure for advancing side area of (a) FSW welded joint and (b) FSP for AlSi9Mg	41
2.26	Microstructure for retreating side area of (a) FSW welded joint and (b) FSP for, AlSi9Mg	42
2.27	Image of (SEM) of the welded joint following second pass of FSW; a) low magnification of SEM micrograph in term of back-scattered electron mode (BSE) of weld nugget exhibits weld, that is free of defects and dispersement of Ti in weld nugget, b) BSE-SEM image from joint interface manifest formation cracks and interlayer, and c) BSE-SEM shows presence image of Ti fragment in weld nugget	45
2.28	EBSD scan following first pass of Al/Ti FSW and related Orientation Imaging Microscopy (OIM) analysis shows a) IPF with grain boundary map, b) distribution map for grain boundary character and c) Grain Orientation Spread (GOS) map of weld for the middle of the cross-section	46
2.29	Image of EBSD scan following second pass for Al/Ti FSW and OIM analysis Shows a) IPF plus grain boundary map, b) distribution map of grain boundary character and c) GOS map of weld of the middle cross-section	47
2.30	Graph above shows True stress vs. true strain plot for the welds at produced different pass of the weld revealing a difference in term of tensile strength and ductility, the highest tensile property being shown of the weld after second pass	48
2.31	Comparison done in graph form for a) distribution of grain size b) misorientation angle distribution of welds for first and second pass with optimized process variable that shows Gaussian grain size distribution and consist of mean for high and low angle of misorientation.	49
2.32	Surface appearance and cross section of weld produced with number of cycles respectively in macroscopic view: AS - advancing side and RS - retreating side	50
2.33	Microstructures of advancing sides for the joints welded by (a) 1 cycle, (b) 2 cycles and (c) 3 cycles	51
2.34	Orientation of colour maps of centre SZ for (a) 1 cycle, (b) 2 cycles and (c) 3 cycles	52

3.1	Flowchart for BFSW process	56
3.2	Dimension of workpiece	57
3.3	Dimension of tool	58
3.4	Plates in butt joint	59
3.5	Hardness mapping for sample	60
3.6	Microhardness Tester machine	61
3.7	Optical microscope (OM)	62
3.8	Scanning electron microscope (SEM)	63
3.9	ImageJ software	63
3.10	Line matching according scale line	64
3.11	Information display regarding the scale	64
3.12	A long yellow line drawn	65
3.13	Display of information regarding the length of yellow line drawn	65
3.14	Formulae to calculate the average grain size	65
3.15	Electronic scale	66
3.16	Water filled inside beaker	66
3.17	Sample placed on tissue cloth	66
3.18	Drawing of ASTM E8/E8M standard for tensile testing	67
4.1	Welded sample A) One pass B) Two pass C) Three pass	68
4.2	Microhardness graph for one pass	74
4.3	Microhardness graph for two pass	78
4.4	Microhardness graph for three pass	81
4.5	Graph of Average Ultimate Tensile Strength (Mpa) vs no of pass	83

LIST OF ABBREVIATIONS

CFSW	-	Conventional Friction Stir Welding
FSW	-	Friction Stir Welding
FSP	-	Friction Stir Processing
TIG	-	Tungsten Inert Gas Welding
MIG	-	Metal Inert Gas Welding
BFSW	-	Bobbin Friction Stir Welding
AA 1100	-	Aluminium Alloy 1100
GMAU	-	Gas Metal Arc Welding
RSM	-	Respond Surface Method
TWI	-	The Welding Institute
BM	-	Base Metal
SEM	-	Scanning Electron Microscope
OM	-	Optical Microscope
TEM	-	Tunneling Electron Microscope
XRD	-	X-ray Diffraction
AS	-	Advancing Side
RS	-	Retreating Side
TMAZ	-	Thermal Mechanical Affected Zone
SZ	-	Stir Zone
NZ	-	Nugget Zone
RPM	-	Revolution per minute
ASTM	-	American Standard Testing of Material
UTM	-	Ultimate Tensile Machine
ANOVA	-	Analysis of Variance
SMAW	-	Shielded Metal Inert Gas Welding

HAZ	-	Heat affected zone
DCZ	-	Dynamic recrystallization zone
GBCD	-	Grain boundary character distribution
SRX	-	Static recrystallization
EBSD	-	Electron backscatter diffraction
BSE	-	Back-scattered electron mode
IPF	-	Inverse pole figure
OIM	-	Orientation Imaging Microscopy
GOS	-	Grain Orientation Spread
UTS	-	Ultimate tensile strength
MAD	-	Misorientation angle distribution
DRV	-	Dynamic Recovery
CDRX	-	Continuous Dynamic Recrystallization
FE-SEM	-	Field emission scanning electron microscope
FAZ	-	Filling Affected Zone
IMCs	-	Intermetallic
BUE	-	Built-up edge
WZ	-	Weld zone

LIST OF SYMBOLS

°C	-	Degree Celsius
MPa	-	Mega Pascal
mm/min	-	Millimeter per minute
µm	-	Micrometer
kN	-	Kilo Newton
kgf	-	Kilogram force
N	-	Newton



اونيورسيتي تيكنيكل مليسيا ملاك

UNIVERSITI TEKNIKAL MALAYSIA MELAKA

CHAPTER 1

INTRODUCTION

1.1 BACKGROUND STUDY

In this current modernization era, manufacturing industries need to enhance the manufacturing process used in order to produce a product that have high strength and less in defects. One of the crucial part in manufacturing process is joining process. Most common joining process involves welding process. Welding process is widely used for many applications such as for manufacturing of marine transports, automotive and aerospace. Welding process offers permanent joint with a high strength.

Friction stir welding (FSW) is one of most significant joining process. It is known as a solid state joining process. It was founded by The Welding Institute (TWI), which located at United Kingdom in 1991 (Fuse & Badheka, 2019). The working principle of Friction stir welding (FSW) technology is by utilizing a non-consumable tool that rotates mechanically. The tool will travel through the area of workpiece that intended to be joined. As the tool rotates at high speed, it produces heat from friction that will make the material softer and closes the weld (Mohammad K. Sued & Pons, 2016). Hypothetically, the grains of material will be transferred and reorganized between two parts of material that intended to be weld without causing it to melt. The advantage of this welding method is producing joint with high mechanical properties, has high efficiency of energy and it can be used to weld many types of aluminium allow as it is a solid state joining process. Other types of welding technique such as Metal Inert Gas (MIG), Gas Metal Arc Welding (GMAU) and Tungsten Inert Gas (TIG) can be categorized under category known as fusion welding. This category is really contrasting in terms of its working principle as in fusion welding will be performed by melting the base metal by supplying heat to

it. Moreover, a filler material is included to the base metal when it undergoes melting process. By doing so, it will will increase the strength to the joint that intended to be weld. According to (Shanavas & Raja Dhas, 2017) for (FSW) process, it does not involve the usage of fusion material. Thus, this process avoids the occurrence if defects at welded areas caused by reaction of metallurgical and deforms in fusion welding process.

Friction stir welding (FSW) process can be grouped into two types, which is conventional Friction Stir Welding (CFSW) and bobbin Friction Stir Welding (BFSW). The categorization is done by referring on the design of tool used. Even though, the process for both types of tool is identical but the method of the joint formed is affected by contrasting approach. This is because, the presence of additional shoulder in (BFSW) that eliminate force of plunge and tilting angle. Figure below shows the difference between two types of tool categorization.

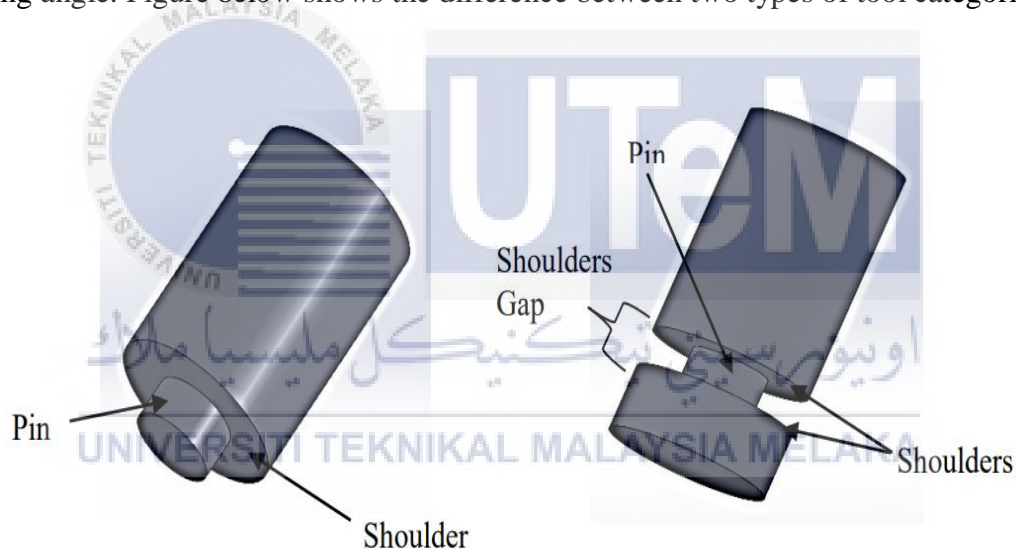


Figure 1.1: Types of FSW. (a) CFSW (b) BFSW (M K Sued, Samsuri, Kassim, & Nasir, 2018)

Friction stir welding is use commonly as solid state joining process to weld aluminum alloy. Aluminum alloy 1100 is widely used in manufacturing of metal sheets as it is light in weight and able to withstand corrosion. Material that has been welded by FSW process will encounter plastic deformation at high temperature that will cause the development of fine and equiaxed recrystallized grains. The presence of fine microstructure by friction stir welding will generate a joint with high strength (Kulkarni, Pankade, Andhale, & Gogte, 2018).

There are defect in welding such as kissing bond, cavity and groove during friction stir welding (FSW). Mostly, this defect is caused by inappropriate of parameter setting or conditional of technological. The presence of defects will affect the mechanical properties of the joints. Thus, repairing welding process of joint is required but there is deficiency in associated studies. Moreover, groove defect is one of the major defects that occurs because of rupture pin tool. The defect will cause degeneration of the weld joint and to the mechanical properties as it has larger size.

Friction stir welding (FSW) is used as repair welding process. To obtain an ideal repair process of welding, the main focus is set on microstructural characteristic and mechanical properties of the joint that undergoes repairing process (H. Liu & Zhang, 2009). (FSW) process used a method for repairing joint for different type of metals such as copper, titanium and aluminum. In addition, the process used to alter the microstructure for material with worn out or corroded surface. Repair welding technique is crucial in manufacturing of products. Structures that undergoes repair process have high fracture toughness, ductility and good strength (Salami, Khandani, Asadi, & Besharati Givi, 2014). For this study, AA 1100 will be weld by using bobbin friction stir welding (BFSW) process in multi-pass way and observation is fully focused on the microstructure evolution.

1.2 PROBLEM STATEMENT

Welding process of aluminium alloy are crucial in manufacturing industry for a wide variety of fields such as automotive, aircraft, marine and for architecture purposes. Aluminium alloy possess vital properties such high machinability, light in weight, high ductility, good weldability and recyclability. Furthermore, it has high resistance towards corrosion. In this research, the material used is an Aluminium alloy 1100 (AA 1100) and is known as wrought alloy whereas its composition is about 99.00% made up of aluminium. It is also known as non-heat treated alloy and its strength is fabricated by alloying the aluminium with other elements. AA 1100 will undergo strain hardening or cold working to acquire its strength.

Purpose of this study is to perform practical study on repetitive welding by using bobbin friction stir welding (BFSW) on aluminium alloy 1100. The main concern is to identify whether multipass or repetition (BFSW) process can change material characterization for improving the weld joint produced or not. If multipass method can improve the weld joint, thus need to discover at which number of pass can improve or deteriorate the weld joint produced.

Furthermore, another aspect is for determining ability of repetition welding in term of repairing process. As the material that undergoes multipass welding technique, number of passes will influence the rejoining of weld. By performing this study, identification for occurrence of rejoin weld at which number of pass can be carried out. It was found that there is defect on welded specimen after BFSW process such as open tunnel. This caused by insufficient heat during process (M.K.A.M. Kassim, M.K. Sued & D.J. Pons 2019) and ineffective stirring between advancing side and retreating side (Tamadon, Pons, Sued, & Clucas, 2018). The problem statement is whether by performing multipass BFSW joining can reduce defects at surface joining by improving the material readiness and provide heat that will 'soften' the material.

By conducting this study, relationship between mechanical property of weld joint and metallurgical property for multipass will be discovered. Multipass will cause change in microstructure for the weld joint thus by correlating metallurgical technique, the relation between mechanical properties and metallurgical property can be determined. It is imperative to study the microstructural characteristic as it can indicate the variation in mechanical properties of welded joint. Thus, this study is carried out to gain more information and comprehension

regarding of repetitive welding by using (BFSW) process on Aluminium alloy 1100. It is vital for this research to be conducted as it is major impact to the propulsion of multi-pass (BFSW). Expansion of this understanding is important to advance, asses and exhibit the potential and also the advantage of utilizing bobbin friction stir welding (BFSW) and finally to obtain usefulness from the improved potential that it provides.

1.3 OBJECTIVE

The objectives of this study are:

1. To analyse the microstructure evolution for multipass bobbin friction stir welding by correlating with metallurgical testing method.
2. To identify the relationship between mechanical properties of material and multipass BFSW welding.
3. To recommend a solution of multipass BFSW based on metallurgical analysis.

1.4 SCOPE OF RESEARCH

The scope of this research is to study the the impact of multipass of bobbin friction stir welding (BFSW) process on aluminium alloy 1100. This research focus mainly on microstructural evolution at end of welding process. Bobbin friction stir welding (BFSW) used for as joining process for AA 1100. The welding process is done in multipass on the workpiece. For this welding process, parameter of the machine such welding speed (mm/min) set at 105 (mm/min) for one pass, 155 (mm/min) for two pass and 205 (mm/min) for three pass. Rotational speed of bobbin tool (rpm) is set constant at 900 rpm throughout the study for each pass. Before testing, the sample will be cut into small parts. The quality of weld will be analyzed in terms of hardness by microhardness test machine and tensile testing. The sample undergoes three processes such grinding, polishing and etching in order to obtain its detailed microstructure. Polishing is done on specimen to get a smooth surface by using abrasive silicon carbide paper with fine scale. Then, etching process is done after polishing by utilizing chemical solution, keller reagent. Both of this process is crucial to get image of a perfect microstructure for analysis purpose. As main concern is on the microstructural evolution on the surface of workpiece, it will be investigated by optical observation. Furthermore, optical microscope (OM) and scanning electron microscope (SEM) used to magnify the image of microstructure in detailed manner in order to carry out further analysis.

1.5 SIGNIFICANT OF STUDY

Bobbin stir friction welding (BSFW) is an effective welding method as it consumes less energy and has capability to perform welding without any fillers. Thus, it has high demand in manufacturing industry such as automotive industry. It is a suitable joining process for producing good quality of weld without defects such as porosity and it is also fully automated. As the process is fully automated, it contributes to high productivity, reduce necessity of manpower for handling purpose and decrease cost of labor. The process is considered as environmentally friendly and does not possess threat towards human's health. (BSFW) process is predominantly used for welding thin sheet of material. High quality of weld promises a strong joint that have good strength and longer durability. In conclusion, this study is crucial to be carried out for analyzing the microstructure evolution on aluminum alloy 1100 due to multipass and to discover relationship between mechanical property and metallurgical property of weld joint produced to increase the quality of weld produced by multi-pass of (BSFW) process.

CHAPTER 2

LITERATURE REVIEW

This purpose of this chapter is to present a detailed explanation in a sequential order from the about previous studies and researches. It will provide and analyze the results and data about this project to acquire comprehension in composing the methodology

2.1 DEFECTS OF FRICTION STIR WELDING (FSW)

In initial step of (FSW) process, tool that is spinning happens to be plunged within the abutting edges of material that need to be welded. The tool rotates at high speed and produce heat as result friction of contacting with surface of workpiece. It will stir the workpiece in way of advancing side (AS) to the retreating side (RS).

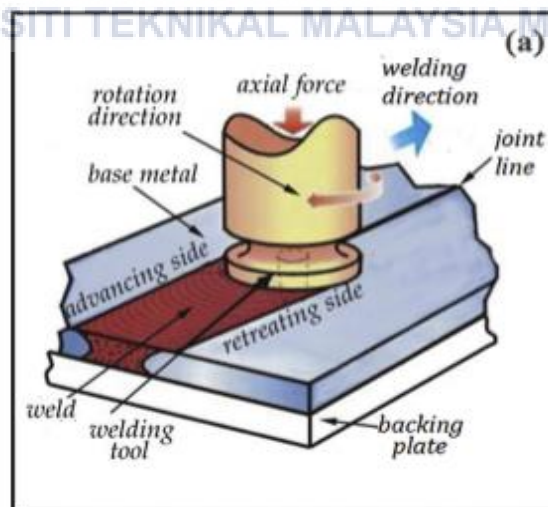


Figure 2.1: Schematic drawing of (FSW) process (Padhy, Wu, & Gao, 2018)

Currently, top sector of industries such as automobile and marine have implemented the usage of friction stir welding (FSW) with a perseverance understanding of element that causes formation of defect. Common defects in (FSW) such as kissing-bond, tunneling, incomplete root penetration and joint line remnant are contrary when compared with defects of conventional fusion welding. Usually, the defects occurs when production of heat is insufficient, movement of material is inappropriate consolidation of material behind the pin. The quantity of heat produced and stirring of material affected by some parameters such as tool rotation, tool design, depth of tool plunge, tool pin offset and position of workpiece. The elements will subsequently cause formation of defects if there is lack of understanding regarding it.

Presence of defect occurs frequently in dissimilar alloys when welded by friction stir welding (FSW). This problem take place as the distinct in the temperature of softening, metallurgy and thermal conductivity that caused uneven distribution of heat. Defects in weld will make the joint weak and easily rupture when force applied on it over time. It is a great obstacle to produce joint with absence of defect through (FSW) process. According to researches, they studied the impact of (FSW) parameter on formation of defect called as kissing bond during welding of aluminium alloy. Their researches proved that rise in transverse speed and insufficient of tool plunge depth. Heat generated from the tool will tend to directly soften the material. Nonetheless, the excessive heat produced doesn't improve the quality of joint. So, proper input of heat is crucial in producing joint with good quality (Khan, Khan, Siddiquee, Al-Ahmari, & Abidi, 2017). Figure below shows kissing bond defect under scanning electron microscope.

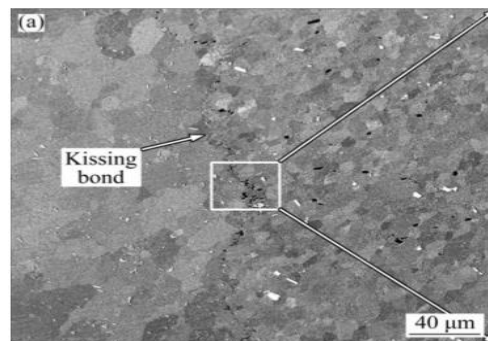


Figure 2.2: Scanning electron microscope image of kissing bond defect (Khan et al., 2017)

In recent study, investigation have been carried out to determine the effect of two parameter on the formation of defects such as kissing bond and tunneling defect. Purpose of this investigation is to gain knowledge on how the both parameters can lead to occurrence of the defects mentioned. By doing so, corrective steps can be taken to prevent the defects (Khan, Siddiquee, Khan, & Shihab, 2015)

A joint with a high strength can be produced if the surface of workpiece is clear and with absence of oxide layer. The layer of oxide present on surface of a material will affect the affect the mechanical properties. Defect such as joint line remnant also known as “entrapped oxide defect” and it will occur as formation of persistent oxide layer. For this issue, a zero joint line appears if the metallurgical bond does not be found beside the defect. Insufficient deformation at the contacting surface between two materials that situated in compressed manner to create a joint will lead to formation of joint line remnant. The defect is made up of arrangement of oxides that is visible from macrostructure analysis. It can be recognized by using either computational method or by conducting experiment. Previously, there is an increase in number of studies carried out regarding initial surface oxide layer reaction during welding process and its impact on creating a weld that possess joint line remnant defect (Dialami, Cervera, Chiumenti, & Segatori, 2019). Figure 2.3 below shows macrograph of joint line remnant.

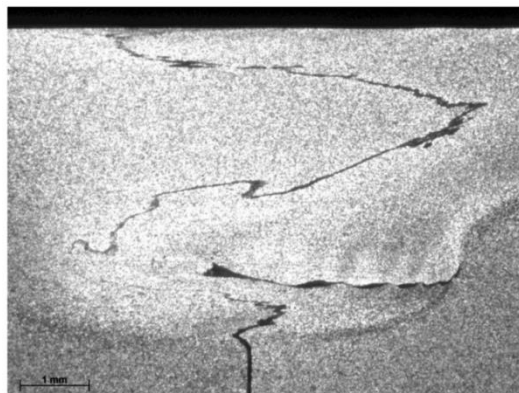


Figure 2.3 : Joint line remnant in (FSW) by macrograph (Dialami et al., 2019)

Another defect that occurs usually in (FSW) process is known as tunneling defect. This defect will affect the strength of the weld and deteriorate the weld quality and defined as wormhole defect. Tunneling defect cannot be seen as it generated under the surface on the welded area. Inappropriate selection of parameter such tool design and transverse speed will cause formation of tunneling defect.



Figure 2.4: Tunneling defect (Khan et al., 2015)

Sufficient knowledge is necessary regarding different types of FSW defects in order to develop the process to be a dependable welding process.

2.1.1 REPAIR PROCESS IN WELDING

A good welding is judged in term of its appearance and mechanical properties. Presence of defect in welded areas will cause bad appearance and low surface finish as defected weld tend to possess disruption on its surface. Therefore, repair process is carried to modify the joint in order to increase the weld quality. In this study, analysis of repair process is done for fusion welding and solid state welding. Repair welding can be used for repairing of weld defects, repairing of failed parts and repairing of worn parts (Salami et al., 2014).

2.1.2 REPETITION METHOD IN FUSION WELDING

Repetitive method used for repair weld of construction steels such as for making submarines and ships able to deal the potential of the joint that undergoes repair process. For example, naval platform such as aircraft carrier will face deterioration at its structure such as corrosion. This problem occurs commonly as the steel tend to corrode as interact with sea water. The metal will oxidized by producing electrons to surrounding by existing as anode. Corrosion has affected the metallic structure for oil and gas companies throughout the world. It can be classify as internal and external corrosion. Naval platform will face external corrosion problem (López-Ortega, Bayón, & Arana, 2018). Thus, this problem creates the requirement of welding process for repair of the structures that underwent deterioration.

Metal will consequently will encounter changes in term of its temperature and mechanical stress as repetitive weld done to repair at constant location that have impact on properties of material. The repetitive weld repair results in growth of grain, formation of high residual stress

and weakening of base metal that can implicate decrease in strength, toughness and increase in fatigue. Previous studies has proved that repair welding can worsen the residual stress at the joint. For short repair, calculational modelling has recommended increase in value of tensile residual stress transverse (Elcoate, Dennis, Bouchard, & Smith, 2005). Repeated weld repair has been proven to have influence on the microstructural and mechanical properties of a material.

Workpiece with high thickness can be weld by using repetitive tungsten inert gas (TIG) welding by including a filler material. This process involves demanding of edge preparation and certain value of welding passes that can cause rise on residual stress and deformation. For example, a weld joint is formed by repetition of thirteen times by utilizing 316L stainless steel filler rod with diameter of 3mm. The result of research shows that welded area that went through thirteen pass has higher hardness compared with activated tungsten inert gas (ATIG) as implemented of thermal cycle at interface of overlaying for the weld areas. (ATIG) has been proven to possess decrease in hardness as it underwent cooling at slow rate when compared to repetitive of (TIG) process (Ganesh, Balasubramanian, Vasudevan, Vasantharaja, & Chandrasekhar, 2016).

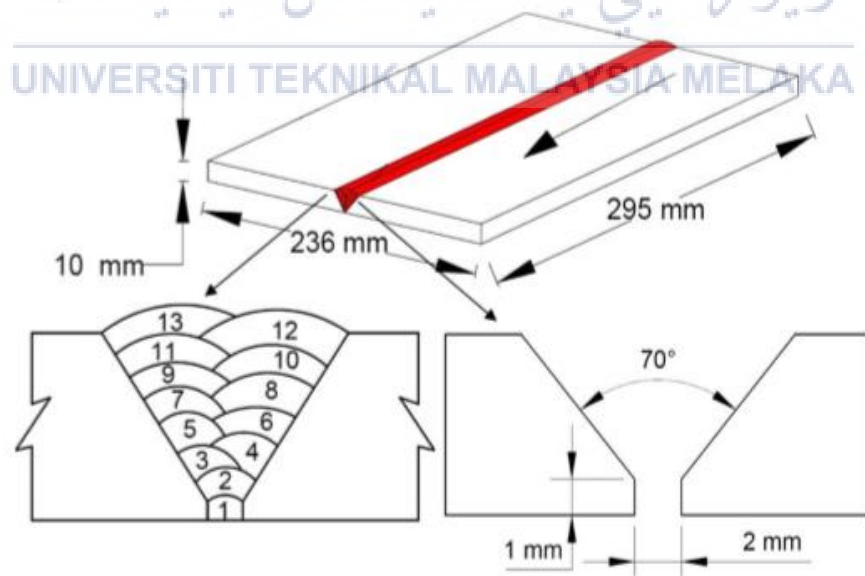


Figure 2.5: Schematic drawing of thirteen passes of 316L stainless steel filler rod (Ganesh et al., 2016)

A study was conducted on repairing joint for offshore pipeline by using gas metal arc welding (GMAW) and shielded metal arc welding (SMAW). Different type of case is studied by performing single partial repair weld, double partial repair weld, single full repair weld and double full repair weld. In single repair, the workpiece will undergoes one cycle of weld and two rounds of same weld process for double repair. Samples were compared with another sample of original welding process Table 2.1 and 2.2 below shows the welding parameter of (SMAW) and (GMAW).

Table 2.1: Parameter of welding for (SMAW) (Zeinoddini, Arnavaz, Zandi, & Vaghasloo, 2013)

	PASS 1	PASS 2	PASS 3	PASS 4
Electrode AWS class.	E7016G	E7016G	E7016G	E7016G
Electrode dia. mm	4	4	3.2	3.2
Current & polarity	AC	AC	AC	AC
Avg. current A	138	144	104	109
Avg. voltage V	25	24	21	22
Avg. travel speed mm/s	9.2	8.1	11.1	9.8
Inter pass temp. °C	52	87	168	203

Table 2.2 : Parameter of welding for (GMAW) (Zeinoddini et al., 2013)

		PASS 1	PASS 2	PASS 3	PASS 4	PASS 5	PASS 6
Electrode AWS class.		E7016G	E7016G	E7016G	E7016G	E7016G	E7016G
Electrode dia.	mm	2.6	3.2	4	4	3.2	3.2
Current & polarity		AC	AC	AC	AC	AC	AC
Avg. current	A	72	103	141	143	105	105
Avg. voltage	V	21	22	24	25	22	22
Avg. travel speed	mm/s	4.2	6.8	8.1	8.3	8.9	9.2
Inter pass temp.	°C	107	133	180	202	185	193

Figure 2.6 below shows the profile for original, partial repairing and full repair weld.

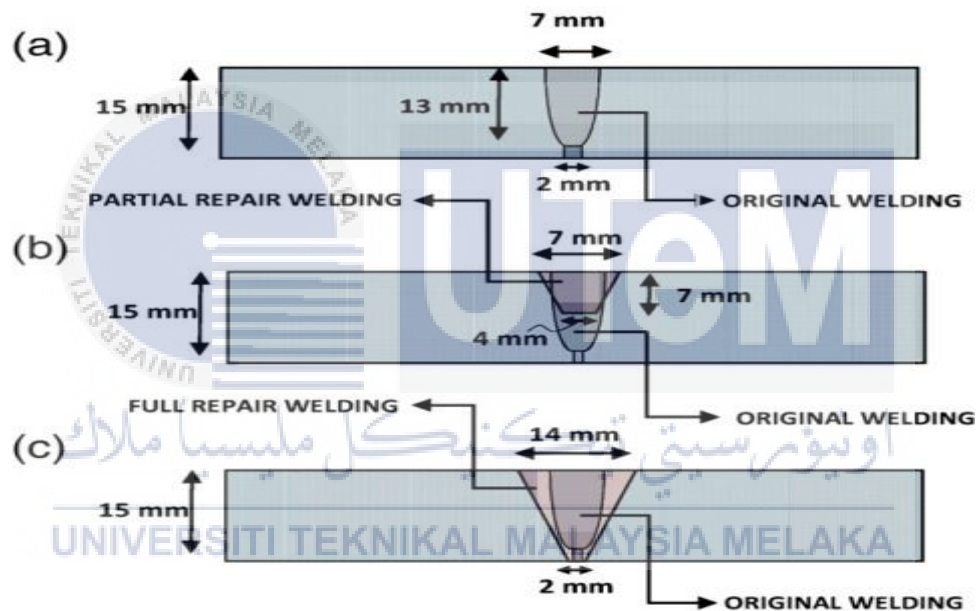


Figure 2.6: Weld passes of profile for (a) original welding, (b) partial repair weld and (c) full repair welding (Zeinoddini et al., 2013)

The sectional areas are then tested by using sectioning technique to measure the residual stress. The result of investigation exhibit increase in tensile stress for single full and partial weld repair at the welded area. Partial repair weld possessed high transverse tensile residual stress in contrast with full weld repair and original welding (Zeinoddini et al., 2013).

2.1.3 MULTIPASS FOR SOLID STATE JOINING WELDING

Solid state joining process such as friction stir welding utilize multipass method for repairing the welded areas. It is known as solid state joining process as absence of melting of material during welding process. Currently, a study carried out to investigate the multipass for friction stir welding (FSW) process on different aluminium alloy 6061. The study is mainly about impact of multipass on the mechanical and metallurgical properties. According to (Singh, Singh, Sandhu, Khan, & Singh, n.d., 2017) double pass friction stir welding has high tensile strength compared to single pass friction stir welding at the end of experimentation. There are some defects formed and grain structure is not fine for single pass friction stir welding. The defects created from single pass can be prevent by utilizing double pass method. This technique enables generation of grain to be more refined and decrease in size of grain. Furthermore, workpiece that experience double pass FSW has high tensile strength than single pass FSW. Moreover, double pass friction stir welding produced specimen with high micro hardness in contrast with single pass friction stir welding. Defects that generated from single pass can be eliminate by utilizing double pass friction stir welding. This method is effective as the double pass friction stir welding will cause the grains become much finer and reducing size of grain.

Furthermore, another research carried out to determine relationship between characteristic of microstructural and fracture toughness for dissimilar region for one pass and two pass of friction stir welding (FSW). Crack tip opening displacement test carried out for testing of toughness at 0 °C, - 20 °C and - 40 °C. Material used as workpiece for joining is API-5L-X80 steel plates. Dimension of steel plates used is 9.5 and with thickness of 15 mm and rectangle plate (450 mm X 95 mm²) undergoes welding process of one pass and two pass (FSW). Parameter of welding used for this study is shown below in table 2.3.

Table 2.3 : Set up of parameter used during (FSW) process (Avila, Rodriguez, Mei, & Ramirez, 2016)

Mechanical properties and average of the FSW parameters. T: Temperature, YS: Yield strength, TS: Tensile strength, EL: elongation.

Mechanical properties				Welding parameters			
T (°C)	25	-20	-40	Pass number sequence	Tool pin length (mm)	Downward force (kN)	*Heat input (kJ mm ⁻¹)
YS (MPa)	593 ± 21	626 ± 45	609 ± 5				
TS (MPa)	658 ± 34	691 ± 1	695 ± 1	P/1	9.5	34	2.1
YS/TS (%)	90	91	88	P/2	6.1	29	1.8
% EL	17 ± 1	14 ± 3	16 ± 1				

Samples that experienced one pass and two pass is tested by using hardness map. By using hardness map, actual size of distinct macrostructural areas and dispersion of hardness. Joint welded by one pass possess constant microstructure than two pass joint. Two pass joint has softening via immense area, which comprise situated at heat affected zone (HAZ) and stir zone (SZ). (HAZ) of second pass causes softening as temperature under critical restriction. This lead to absence in transformation in microstructure that is softened and only hardening maps can identify this specified area. Figure 2.7 below shows hardness maps of cross section for one pass and two pass (FSW) process.

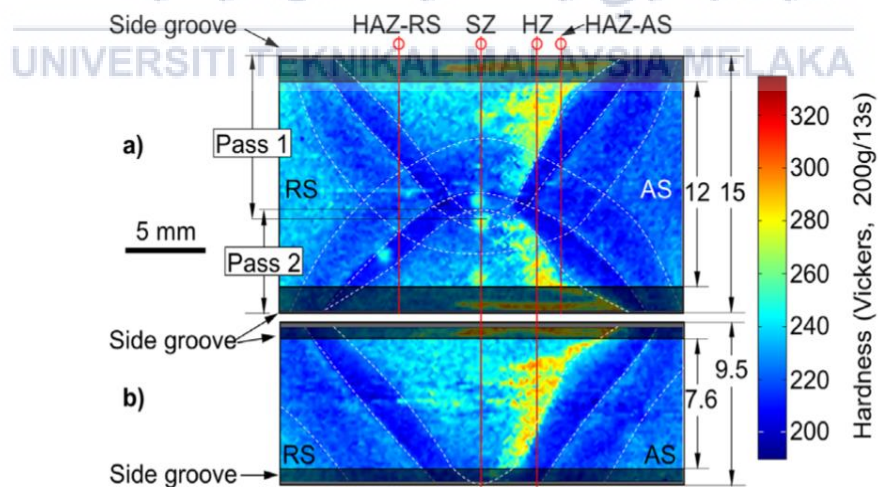


Figure 2.7: Hardness maps of cross sectional area for: (a) two- and (b) one-pass welded joints (Avila et al., 2016)

Heat affected zone is the region where notches located at advancing side (HAZ-AS), retreating side (HAZ-RS), hard zone (HZ) and stir zone (SZ). Machined part at the material is shown by the transparent rectangle that is in dark colored from side grooves. Macrostructural areas indicated by dashed lines. Friction stir welding (FSW) can cause formation of variety in microstructure. Hard zone (HZ) of joint that undergoes one pass weld has the smallest value in toughness (Avila et al., 2016).

2.2 IMPACT OF PROCESS PARAMETER

Friction stir welding (FSW) process affected by several parameters such tool design, speed of spindle and travelling speed of tool. Understanding of these parameter is vital for producing a weld joint with high quality (Shashi Kumar, Murugan, & Ramachandran, 2019). The parameter need to be set up according to type of material of the workpiece that undergoes welding process. Currently, direct guidelines on rotational speed and travel speed ratio is unavailable for producing a weld with good mechanical property. Researches regarding of the parameters are carried out by using trial and error method. This method is crucial to produce quality weld and avoid formation of defects. Presence of defects will cause wastage of material that also create loss in terms of cost. To attain a good weld, it is necessary to carry out studies on causes of defect formation and come up with a compatible setting of parameter. The tool will plays important functions such as produce frictional force, encompass plastic material under tool's shoulder and control the flow of material. For welding process of thin sheets material, most of the heat production from tool's shoulder. Meanwhile, for workpiece with high thickness, pin of tool generates the heat. Special attribute of pin and on the surface of tool shoulder will assist for production of heat and flow of material (Padhy et al., 2018).

2.2.1 TEMPERATURE

Parameter such as speed of spindle and tool design for friction stir welding (FSW) will impact on distribution on temperature and processing loads. A study is carried out to study the relationship between process parameter and temperature distribution on polycarbonate. Formation of macroscopic defect were associated with characteristic of loads and temperature trend as evolution of critical condition. Temperature of distribution is recorded during the experiment by utilizing IR camera model E60. The camera was located at distance of nearly 300 mm from the contact point between workpiece and tool at an angle of 60 degrees to evaluate the temperature of rear part of tool. Then, the specimen were cut about dimension of (60 mm x 90 mm). The difference in temperature emitted of the surface of polycarbonate is recorded in Figure 2.2.1. For until $T \leq 200$ °C, the emissivity is nearly uniform. Green marks represent larger quantity of temperature that related with decrease in term of emissivity. The emissivity decrease to value of 0.6 for temperature of 360 °C. Quantity of 0.6 is deduced for these condition.

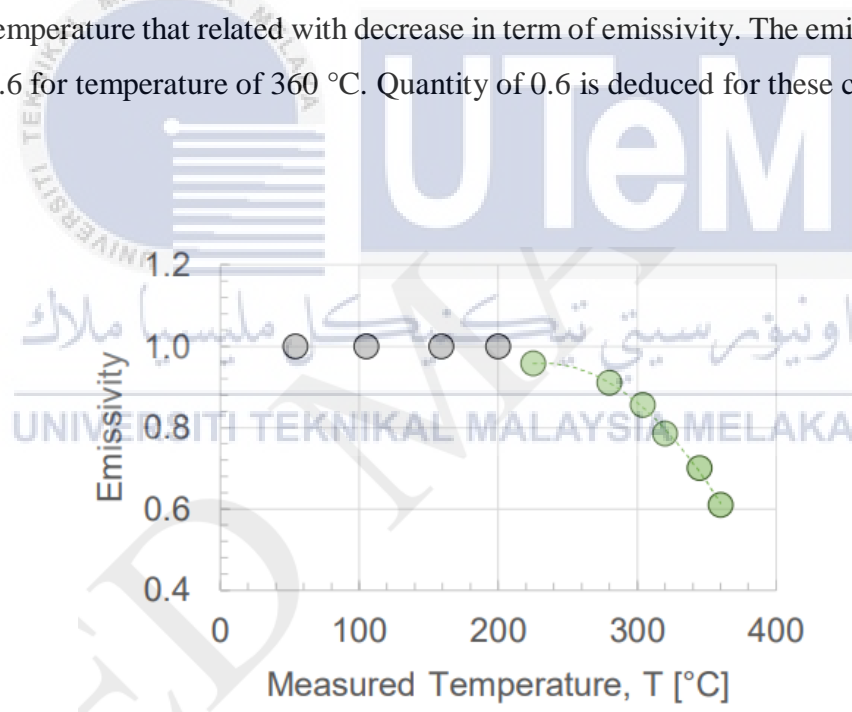


Figure 2.8 : Difference of emissivity with temperature (Lambiase, Paoletti, Grossi, & Di Ilio, 2019)

Aim of this study is to gain knowledge on how process parameters can impact the temperature and processing loads. For this study, welding with elevated speed is used. The welds

were mainly affected by the presence of circular rifts due to unstable process conditions under low welding speeds. According to (Lambiase et al., 2019) high temperature, which even higher than the polymer's degradation temperature and pressure conditions under high welding speeds causes in the generation of built-up edge (BUE) under the shoulder of the tool. By performing welding at higher speed, it increase the temperature at stirred areas. As the temperature increases with higher welding speed that lead to rise of contact pressure that also occurs from rise in heat by frictional force. Polycarbonate will tend to experience thermal deterioration when welding speed is more than 60 mm/min.

2.2.2 MECHANICAL ANALYSIS

Mechanical analysis can be defined a test or investigation that conducted to study and identify the property of material in term of tensile strength and hardness. Usually mechanical analysis is done on welded joint to evaluate its residual stress and strength. When compared with conventional welding process, friction stir welding (FSW) has benefits of producing weld joints that free of defects such as thermal residual stress, porosity and cracking due to solidification. This types of defects occurs commonly in conventional welding due to cooling when the joint formed is change from liquid state to solid state. Material that undergoes (FSW) process will not experience reduction in term of mechanical properties. According to (Devaiah, Kishore, & Laxminarayana, 2018), material that joined by (FSW) process tend to possess good mechanical properties. Generally, almost all researches use traditional technique such as by manipulating one parameter while another parameter is kept uniform throughout the experiment to analyze the impact of process parameter for FSW.

Rotational speed of spindle, which is very fast or very slow will produce weld with low quality as less flow of material and extra exclusion (Verma, Taiwade, Reddy, & Khatirkar, 2018). Proper selection of parameter is crucial to reduce occurrence of intermetallic (IMCs). A research was conducted to weld different types of metal such as Mg-AZ31B and Al-AA6061 by using different rotational speed, which is low, moderate and high. The research is focused on impact of rotational speed on the corrosion resistance of the weld produced. The results that

obtained proved that weld joint produced by high rotational speed has higher resistance towards corrosion. High rotational speed lead to crushing of the particles fully and the grains dispersed were constantly. Coarsening of precipitate when generation of heat at low transverse speed and high rotational speed will increase the resistance towards corrosion for the joint. Weld joint performed at low rotational speed has low strength and hardness as it doesn't not have sufficient time for forming atomic bond between Al and Mg by the frictional heat. Joint weld produced at high rotational speed and transverse is a preferred alternatives as it can cause the increase in hardness of joint and also the tensile strength. Meanwhile, corrosion resistance of a joint can be enhanced by performing weld at high rotational speed and low transverse speed.

According to (Muthu Krishnan, Maniraj, Deepak, & Anganan, 2018), Process parameters in friction stir welding (FSW), which are speed of welding, rotational speed and axial force influence the quality of weld produced. An investigation done to understand the relation between process parameter of (FSW) process parameter and its impact on mechanical properties of weld such as yield strength and tensile strength. Workpiece that used for the investigation are aluminium alloy 6063 and Aluminium 319. Table 2.4 below shows the parameter for the investigation.

Table 2.4 Parameter for FSW welding of AA6063 and A319 (Muthu Krishnan et al., 2018)

Process Parameters	Unit	Symbol	Levels				
			-1.682	-1	0	1	1.682
Tool rotational speed	rpm	<i>N</i>	800	901	1050	1198	1300
Welding Speed	mm/min	<i>S</i>	20	24	30	36	40
Axial Load	kN	<i>F</i>	3	4	5.5	7	8

Welding speed, tool rotational speed and axial load are the parameters set up for the research. The observation is mainly about testing tensile strength, percentage of elongation, hardness and yield strength. Table 2.5 below represent the direct impact of process parameter towards mechanical properties weld from FSW process

Table 2.5: Direct impact of process parameter (Muthu Krishnan et al., 2018)

<i>Direct effects of Tool Rotational Speed</i>		
Lower Parameter Value	Optimum Parameter Value	Higher Parameter Value
<ul style="list-style-type: none"> • Frictional Heat generated is lower. • Higher cooling rate decreases the plastic flow and inadequate bonding • Coarser Grain 	<ul style="list-style-type: none"> • Optimum heat input resulting in finer grains with the increased plastic flow Adequate bonding 	<ul style="list-style-type: none"> • Higher heat input • Slow cooling rate • Metallurgical transformation such as solubilisation, reprecipitation and coarsening of the precipitates.
<i>Direct effects of Welding Speed</i>		
<ul style="list-style-type: none"> • Heat input in SZ is high. • Frictional heat generated per unit length is very high • Coarse grains developed in SZ 	<ul style="list-style-type: none"> • Tool-work interaction is improved. • Frictional heat generation per unit length gets reduced. • Sufficient plastic flow of material in SZ • Fine grains formed 	<ul style="list-style-type: none"> • Material receives less frictional heat • Insufficient plastic flow of material in SZ • Coarse Grains formed • Plasticized material is cooler and less easily forged by the tool shoulder resulting in lack of bonding
<i>Direct Effects of Axial Load</i>		
<ul style="list-style-type: none"> • Insufficient heat due to escape of heat from the upper surface of base plate. • Shoulder was not capable of confining the material within the SZ, a part of material is lost as flash 	<ul style="list-style-type: none"> • Plasticized material from leading edge to trailing edge is confined within the weld cavity. • Heat generation is more • Loss of heat is diminished due to confinement of material within the weld cavity. 	<ul style="list-style-type: none"> • Increased frictional heat generated • Material is lost as flash due to excessive rubbing of tool shoulder and base plate resulting decreased cross sectional area. • More heat loss due to removal of material from base plate with the decreased availability of heat for weld formation • Severe clustering of precipitates

As the welding speed is higher, it brings a detrimental effect on the characteristic of weld. Quality of weld is reduced after the tool has attained the maximum rotational speed

2.2.3 MICROSTRUCTURE ANALYSIS

Friction stir welding (FSW) generated lower amount of heat compared with conventional welding such metal inert gas (MIG) welding and gas tungsten arc welding (GTAW). Thus, (FSW) will enhance the mechanical properties and causes slightly changes in microstructure. A research is carried out to study is done for joining AA 5182 and AA 7075 by (FSW) process by setting under different rotation speed of 980, 1325 and 1800 rpm. The feed rate is set at feed 108 and 233 mm/min. The study is focused on effect of rotation of speed to the microstructure

evolution. Table 2.6 below shows details of rotational speed and feed rate used for the experimentation

Table 2.6: Parameter set up for this investigation (Cetkin, Çelik, & Temiz, 2019)

Stirrer Geometry	Rotational Speed (rpm)	Feed rate (mm/min)
Conical and Triangle	980	108
		233
	1325	108
		233
	1800	108
		233

The construction of the joint welded by (FSW) can be classify as heat affected zone (HAZ), dynamic recrystallization zone (DCZ) zone known as base metal (BM). The construction of the joint welded by (FSWS) can be classify as heat affected zone (HAZ), dynamic recrystallization zone (DCZ) zone known as base metal (BM). Analysis done for these areas in micro and macro size. Figure 2.9 below shows areas in structure of the FSW joint.



Figure 2.9: Zones formed in FSW joint performed (Cetkin et al., 2019)

In this study, AA7075 and AA5182 aluminium alloys were joined using different rotation speeds (980, 1325 and 1800 rpm), feed rates of (108 and 233 mm/min) and stirred pins having two different geometries (conical helical and triangular). Microstructures of welding joints were examined by an optical microscope and a scanning electron microscope (SEM).

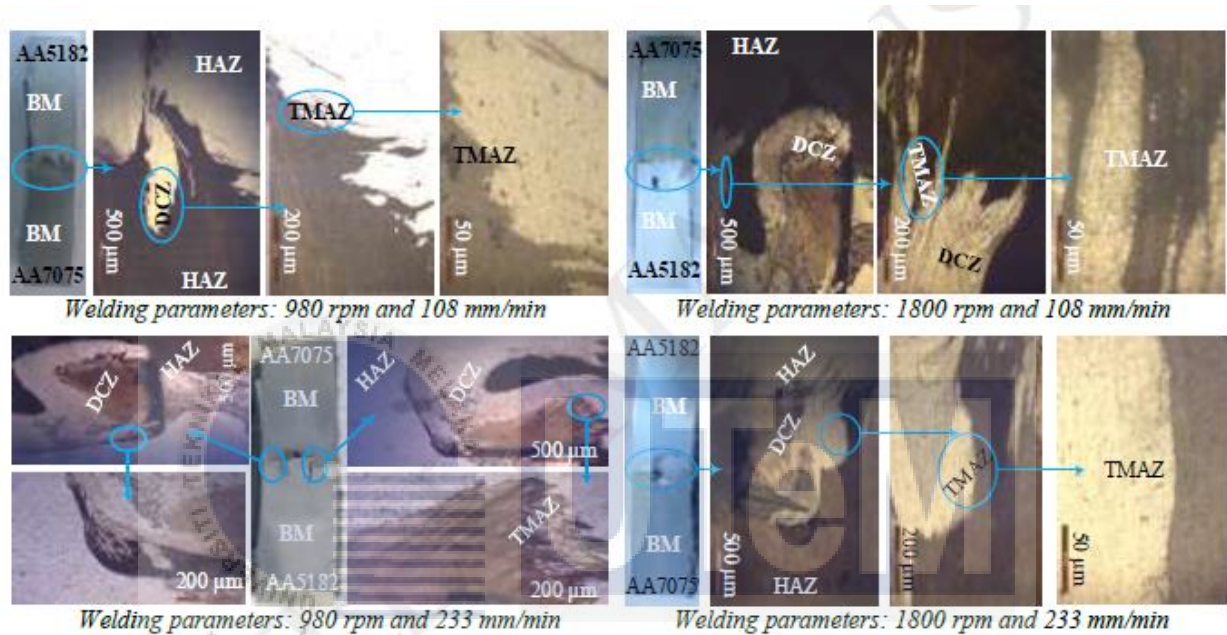


Figure 2.10: Macro and microstructures in (FSW) joints by using conical stirrer pin (Cetkin et al., 2019)

اونيفرسيتي تكنولوجيكا ملسيا ملاك
UNIVERSITI TEKNIKAL MALAYSIA MELAKA

The observation shows the formation of structure known as TMAZ, DCZ, HAZ and porosity in the joint zone formed. These features are affected by parameter such as rotational speed and feed rate. There were presence of wide gaps in the joining zone for the welded sample with rotation speed of 1800 and feed rate of 233 mm/min. For welded sample at rotation speed of 980 rpm and feed rate of 108 mm/min, the microstructure shows less in formation of porosity and the material is suitable for join by extruded.

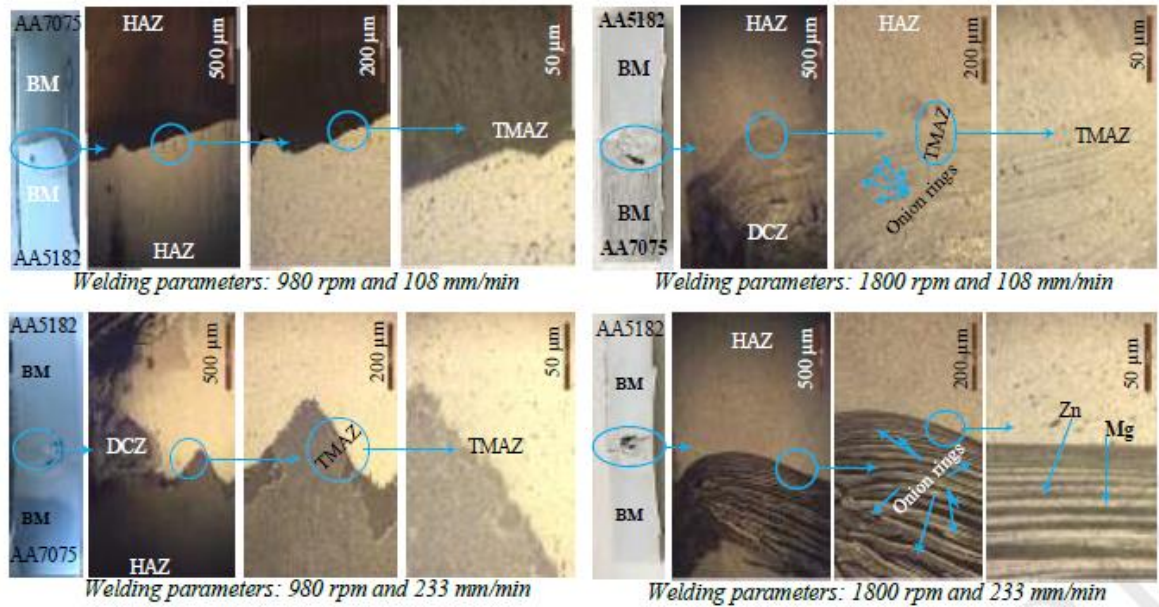


Figure 2.11: Macro and microstructures in (FSW) joints by using the triangular stirrer pin (Cetkin et al., 2019)

In figure 2.11, there is a presence of gaps at center of welding and at the bottom of DCZ areas for AA7075 and AA5182 alloys that joined by using triangle stirrer pin at feed rate of 108 mm/min and rotation speed of 980 rpm. As the feed rate and rotational speed is higher, it will cause the amount of gap at welded joint to be higher. According to (Cetkin et al., 2019), the rotational speed and feed will consequently affects the microstructure of welded joint.

2.3 MATERIAL BEHAVIOUR IN REPAIRING

It is vital to study the material behaviour to analyze the microstructure evolution during friction stir welding (FSW) process in term of heat energy received, presence of contamination and additional material or also known as filler.

2.3.1 HEAT FROM MULTIPASS

As the workpiece undergoes multipass, it will experience higher heat energy compared to single pass. Multipass friction stir welding (FSW), used for obtaining weld joint with high strength. A study carried out for welding dissimilar metals such as AA6082-T6 aluminium alloy and S355J2 + N steel in multipass method.

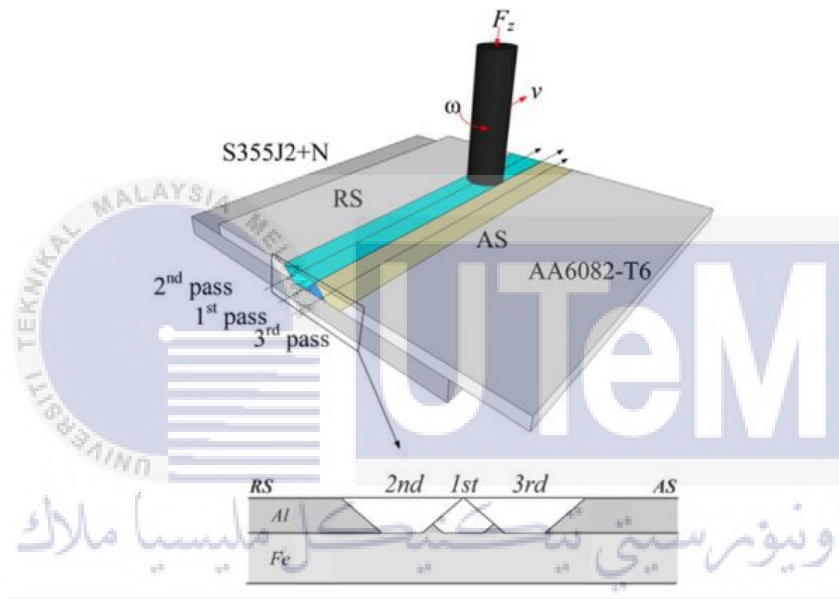


Figure 2.12: Schematic diagram of multipass (FSW) process done (Leitao, Arruti, Aldanondo, & Rodrigues, 2016)

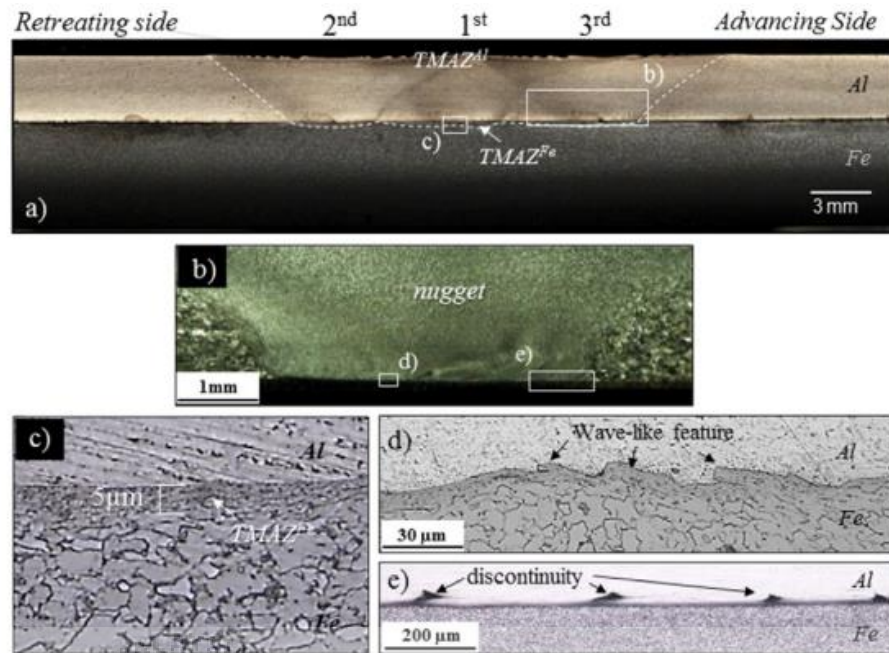


Figure 2.13: Image for transverse cross-section of the weld (a) and enlargement image of the Al-Fe interface (b to e) (Leitao et al., 2016)

In the figure above, the thermo-mechanically affected zone (TMAZ) for the three welding pass are shown in clear manner for the aluminum part with thickness of 5 μm . Three different TMAZ are divided by 2 mm large disconnected area. As for aluminium, it possess extremely refined microstructure as effect of dynamic recrystallization. The starting microstructure for the base material does not affects by the tool for disconnected zones located between the half overlapped nuggets. The microstructure of TMAZ at the steel side of the weld is made up of deformed grains as can be analyzed from figure 2.13c and d. Figure 2.13 also exhibits absence of interlayer and formation of Al-Fe intermetallic. Magnification from figure 2.13e shows the formation of tiny discontinuities, which are dispersed along the interface (Leitao et al., 2016).

2.3.2 PRESENCE OF CONTAMINATION

According to (Vural, 2014), when performing solid state joining or repairing process, presence of contaminants should be eliminated in order to obtain a good metallurgical bonding. In some situations, cleaning process is carried out before conducting welding process meanwhile in other situation, the cleaning work is done to enable the joining of part surface jointly as an important part. In conclusion, surface of workpiece need to be clear from contaminants for enabling better atomic bonding.

A study was conducted to produce aluminium matrix that possess high performance with directionally aligned by utilizing friction stir processing and subsequent rolling. Carbon nanotube (CNT)/ (Al) aluminium has high strength but its elongation of (2-6%) was not acceptable, which occurs due to presence of contamination by aluminium oxide, (Al_2O_3). When FSP method used to produce the CNT/Al composites, it causes presence of contamination in smaller amount and increased size of grain about (0.8–2 μm). The composite tend to have increased in strength and high ductility when aligned (Z. Y. Liu, Xiao, Wang, & Ma, 2013).

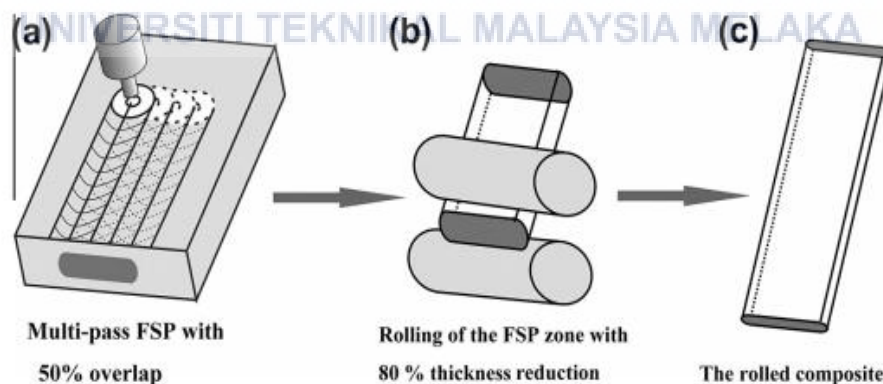


Figure 2.14: –Schematic diagram of making CNT/2009Al composite sequence (Z. Y. Liu et al., 2013)

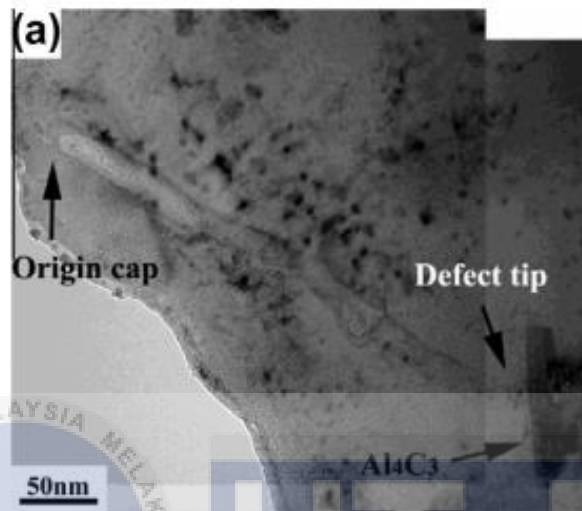


Figure 2.15: Image of TEM for CNT-AL alliance (Z. Y. Liu et al., 2013)

Figure 2.15 exhibit transmission electron microscopy (TEM) image for FSP-rolled 4.5 with vol. % CNT/2009Al composite under high enlargement view. It shows the alliance between CNT wall and Al that has good bonding, which is free of defects and clean from contaminants.

2.3.3 ADDITIONAL MATERIAL / FILLER

Many techniques have been introduced for rectifying defects such as keyhole that generated by rotational tool in friction stir welding (FSW). This technique can be divided into two types, which is a rotational pin used as filler material and tool that is pinless acts as a filler material. A research carried out by using drilling friction stir repairing ((D-FFSR) method to repair occurrence of volume defects for AZ31B magnesium (Mg) alloy.

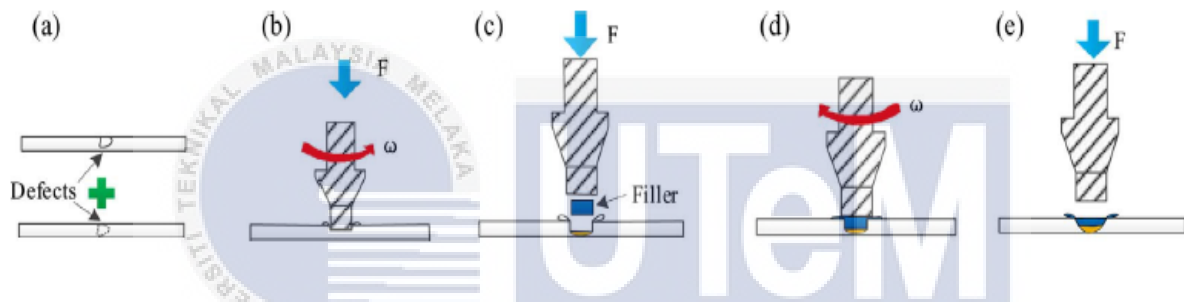


Figure 2.16: Schematic diagram for D-FFSR process: (a) volume defects, (b) stage of drilling, (c) include fillers, (d) stage of filling and (e) stage for retracting (Huang, Ji, Meng, & Li, 2018)

In (figure 2.16 a-c), it shows the defect known as volume defect are machined before adding filler material. This technique involves processes such as drilling, filling and stage of retracting. For this D-FFSR method, two tool which is pinless type with dissimilar diameter is utilized. Pinless tool that possess small diameter is applied to drill a hole in cylindrically shaped as in (figure 2.16b). Then, a filler material that has same diameter with the cylindrically shaped hole is added into the hole (figure 2.16c). Figure 2.16d shows another pinless tool that has bigger diameter will produce heat from frictional force on the material used as filler. Lastly, the retraction of pinless tool will take place and the repairing process is finished successfully.

Joint that produced by D-FFSR can be classified into four areas, which are known as thermo-mechanically affected zone (TMAZ), heat affected zone (HAZ) and stir zone (SZ). There are drilling affected zone (DAZ) and of filling affected zone (FAZ) under (SZ) area.



Figure 2.17: Cross section of repaired joint (Huang et al., 2018)

Figure below shows drift of material inside the groove under this situation. The material will encounter two forces, which is first force known as positive pressure and second force called as friction force. The positive pressure is produced by the side wall from the groove. Friction force occurs between side wall of groove and plasticized material. The filler material will be transfer the material into the middle of FAZ by the resultant force (N) as the tool rotates in clockwise direction. At filling stage, the material that gathered will be higher and partially flow according to the law of least resistance. Moreover, the joint that have undergo repairing process is free from formation of defects (Huang et al., 2018).

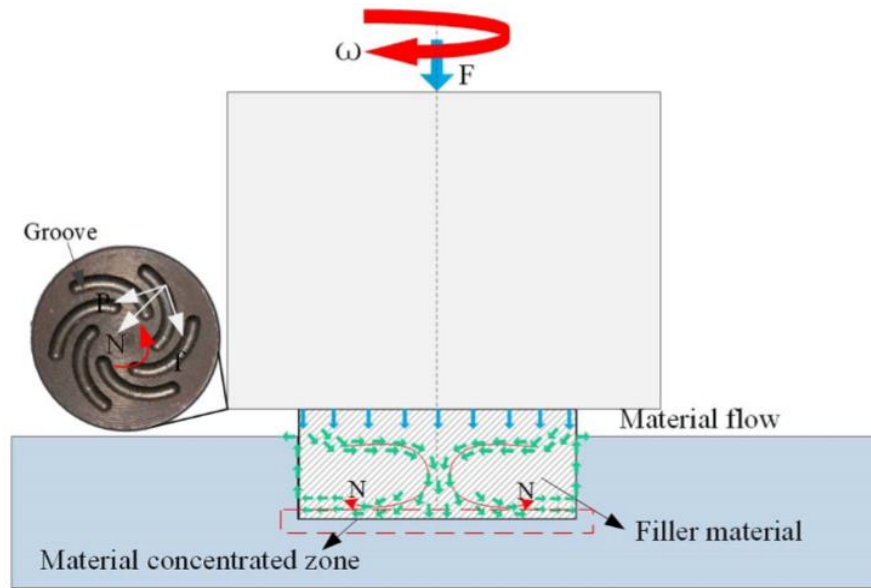


Figure 2.18: Material behaviour at filling stage (Huang et al., 2018)

The material behaviour at filling stage is useful to escalate the height of FAZ. Filling stages were successfully performed to repair this fabricated defect. Moreover, the temperature and effect of forging that take place in filling stage are the vital elements that affects formation of joint. The microhardness distribution of the repaired joint was flat, and an excellent diffusion bonding occurred at the interface between the filler and the base material (BM) under the optimum combinations of a rotational velocity of 1600 rpm, dwell time of 20 s and plunge depth of 0.4 mm (Huang et al., 2018).

2.4 MICROSTRUCTURE EVOLUTION IN WELDING

According (Abd Elnabi, Elshalakany, 2019), friction stir welding (FSW) process involves a rotating tool which plunged in between plates that were clamped. Heat from the frictional force will lead to formation of plasticized region around the rotating tool for producing joint in solid phase. Material that has been welded by using friction stir welding (FSW) will encounter modification in term of this microstructure due to the heat generated between tool and the material that being welded.

2.4.1 EFFECT OF PROCESS PARAMETER

A study done to investigate the impact of parameter set up of welding such as traverse speed (mm/min) on the microstructure evolution. AISI 316L stainless steel and aluminium 5083H321 is used as joining material for this study. By using optical microscope, the macrostructure and microstructure of the welded joint is analyzed. Figure below shows parameter set up for the study.



Table 2.7: Parameter used for welding (Yazdipour & Heidarzadeh, 2016)

No.	Tool rotational speed (rpm)	Tool traverse speed (mm/min)
1	280	160
2	280	200
3	280	250
4	280	315
5	280	160
6	280	160
7	280	160
8	280	160
9	280	160

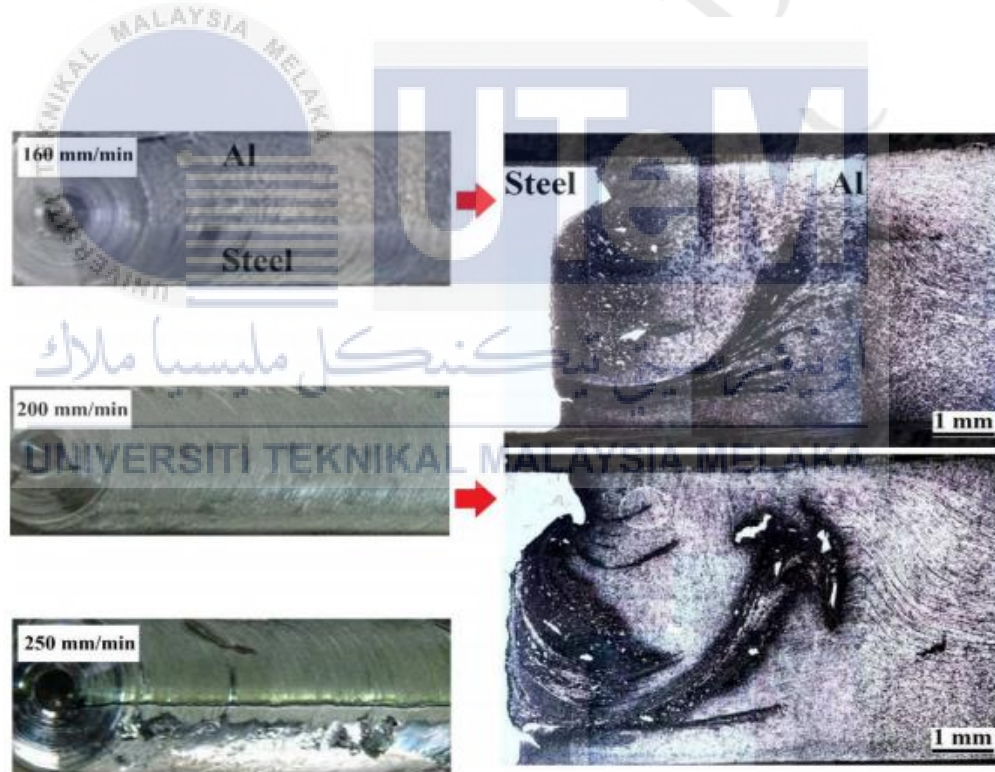


Figure 2.19: Surface of joint and its macrostructure at variation of speed (Yazdipour & Heidarzadeh, 2016)

Figure below shows the impact of traverse speed on tensile strength of the joint in graph for presenting the obtained data. Welded joint at 200 mm/min to 160 mm/min is free of defects. By referring macrostructure, the presence of non – uniformity and coarse particle at stir zone that have been welded at 200 mm/min lead to decrease in tensile strength. Joint that welded at traverse speed of 250 mm/min has formation defects that lowers tensile strength fully. When FSW process carried out at speed more than 315 mm/min, it resulted in breakage of tool pin (Yazdipour & Heidarzadeh, 2016).

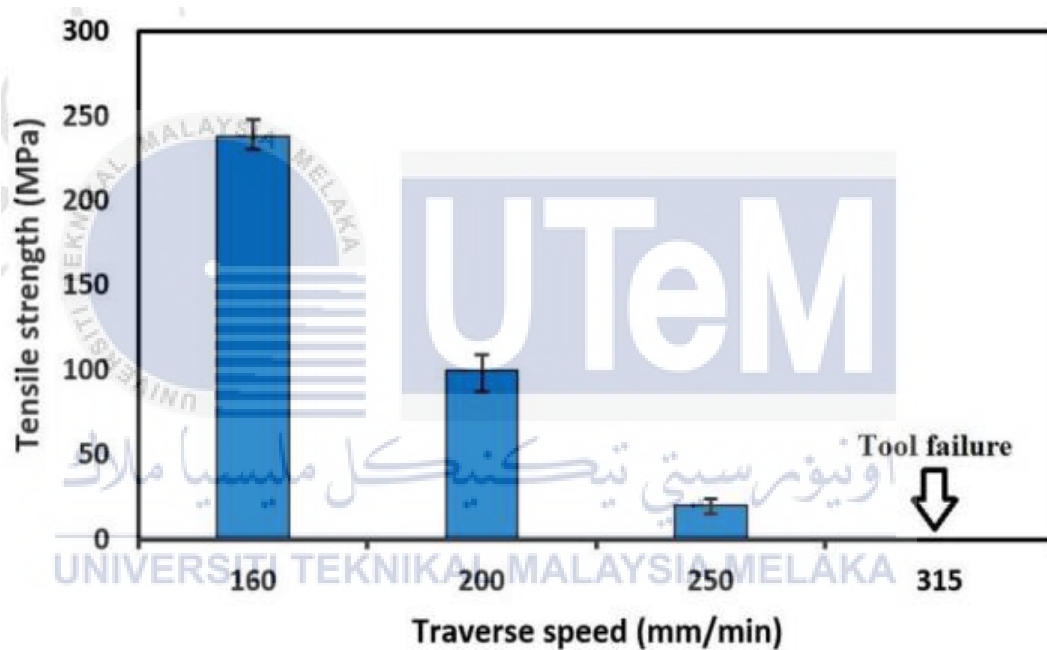


Figure 2.20: The impact of tool traverse speed on the tensile strength for the welded joint (Yazdipour & Heidarzadeh, 2016)

From figure below, there is a presence of micro cracks for the joint that have been welded at 200 mm/min that minimize the tensile strength. During tensile test, micro cracks that formed will grow up in size for a bigger cracks that increase the occurrence of fracture.

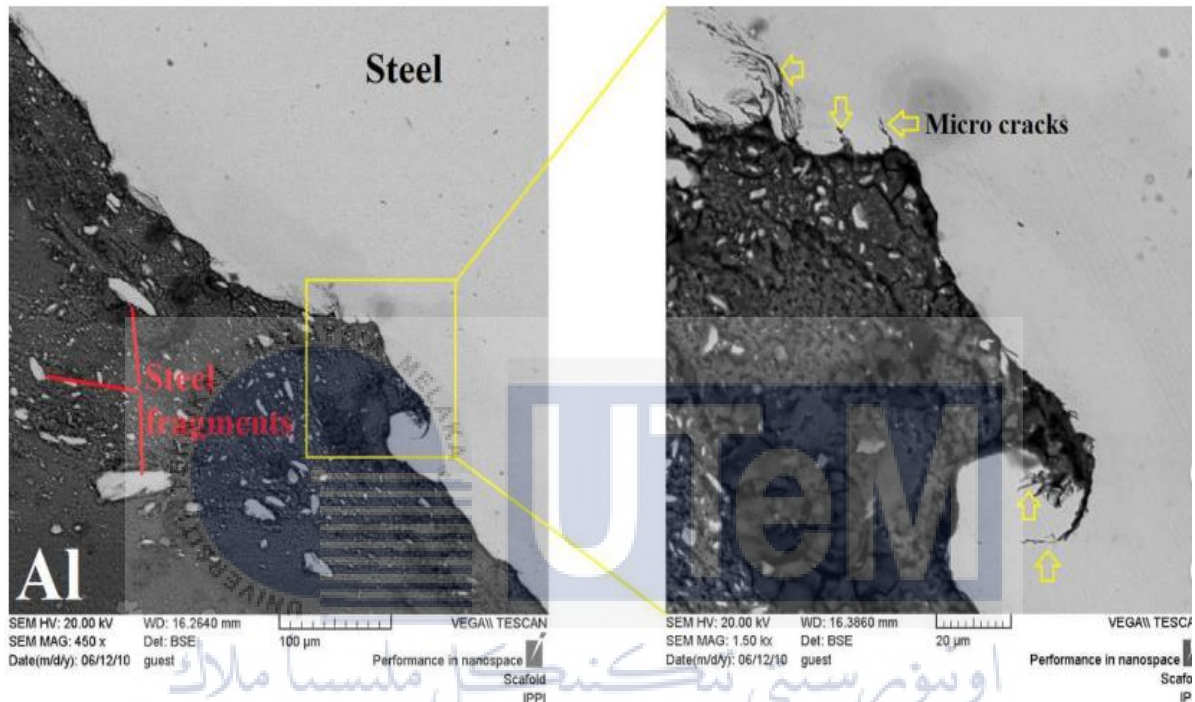


Figure 2.21: Microstructure of joint welded at 200 mm/min (Yazdipour & Heidarzadeh, 2016)

2.4.2 FOR REPAIRING

According to (Węglowski, 2018), friction stir processing (FSP) used for repairing weld joints. This process is mainly used for alteration of microstructure for metallic element on its surface layer. By utilizing this process, fine grain structure and alteration of microstructural can be obtained for cast alloys and to enhance quality of joint that have been welded. Working principle for the friction stir processing (FSP) is similar to friction stir welding (FSW). The main difference in (FSP) process is that it alters the microstructure of workpiece rather than joining together to attain the desired properties of sample by altering microstructure on the surface.

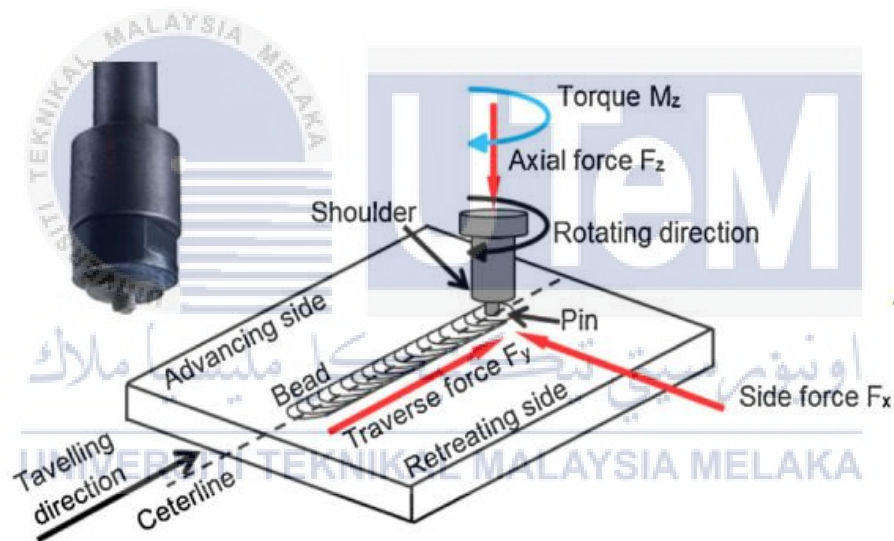


Figure 2.22: Schematic drawing of (FSP) process (Węglowski, 2018)

Working principle of the process is a pin plunged into an altered workpiece that consist of rotating tool adjoin with base metal. As the tool moves in diagonal direction, it produces heat due to frictional force. This contribute to evolution of microstructure as effect from impact cause by plastic deformation and high temperature. Both aspect can be distinguish by heat affected zone (HAZ) and thermos-mechanically affected zone (TMAZ). The material that has underwent

deforming is relocate to advancing side (AS) from retreating side (RS) of tool pin, that causes alteration of solid state for workpiece.

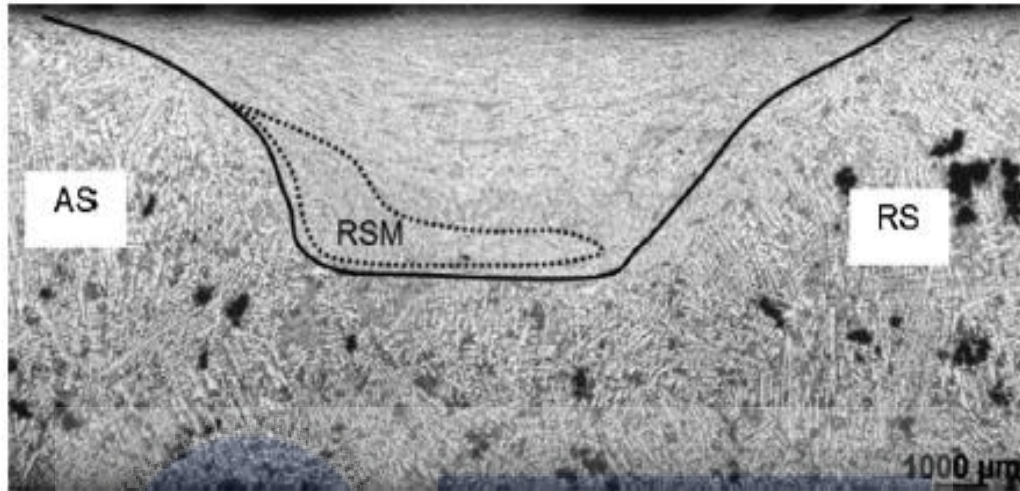
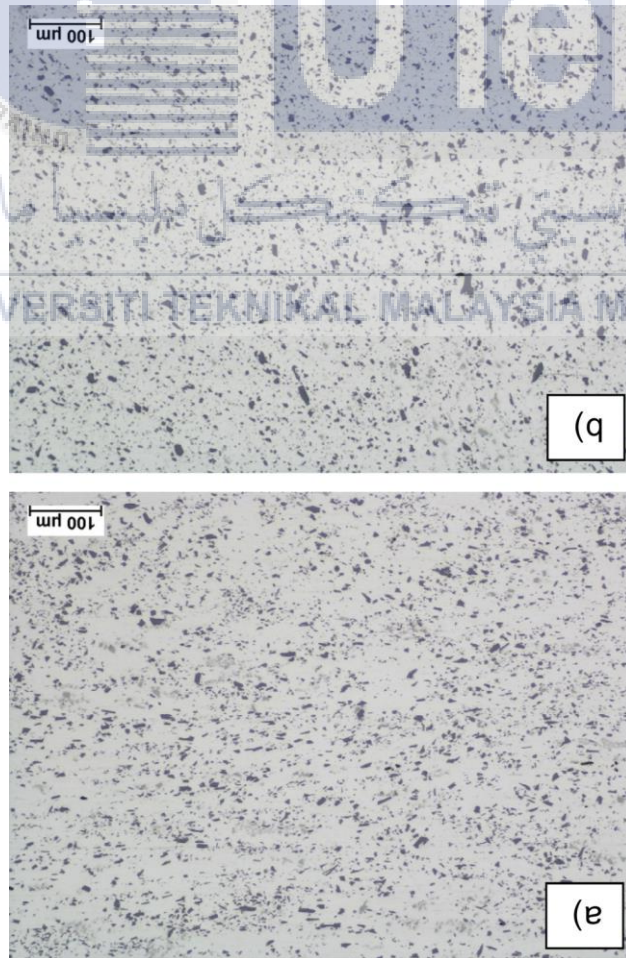


Figure 2.23: Macrostructure of Al-Si alloy that underwent to the (FSP) process(Węglowski, 2018)

The heat generated from frictional force will cause modification of microstructural for the workpiece. An investigation carried out on AlSi9Mg aluminum alloy by using (FSP) process. Its microstructure is analyzed for the joint welded by (FSW) and also by (FSP) process.

Analysis of microstructure is carried out by utilizing light microscope and it shows formation α -Al state in bright manner while Si particles appeared in dark. Si particles have been evenly dispersed in α -Al matrix in the response surface methodology (RSM). The other part of stir zone, which located outside (RSM) region that has experienced deformation towards retreating side (RS). Therefore, initially concentrated of Si particles located inside interdendritic areas have persist while the microstructure more likely to be separated.

Figure 2.24: Microstructure of stir zone for (a) FSW welded joint and (b) FSP for AISI9Mg (Węglowski, 2018)



From the observation carried out, there is deficiency in visible of microstructure's variation for segregate parts which are called as stir zone (SZ), retreating side (RS) and advancing side (AS).

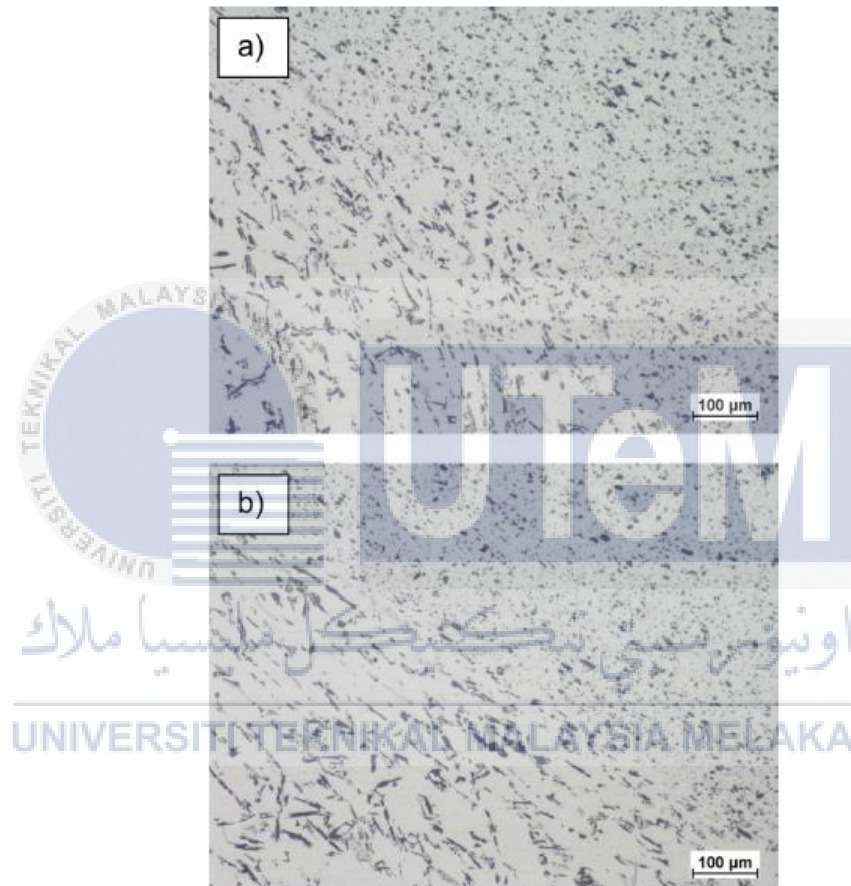


Figure 2.25: Microstructure for advancing side area of (a) FSW welded joint and (b) FSP for AlSi9Mg (Węglowski, 2018)

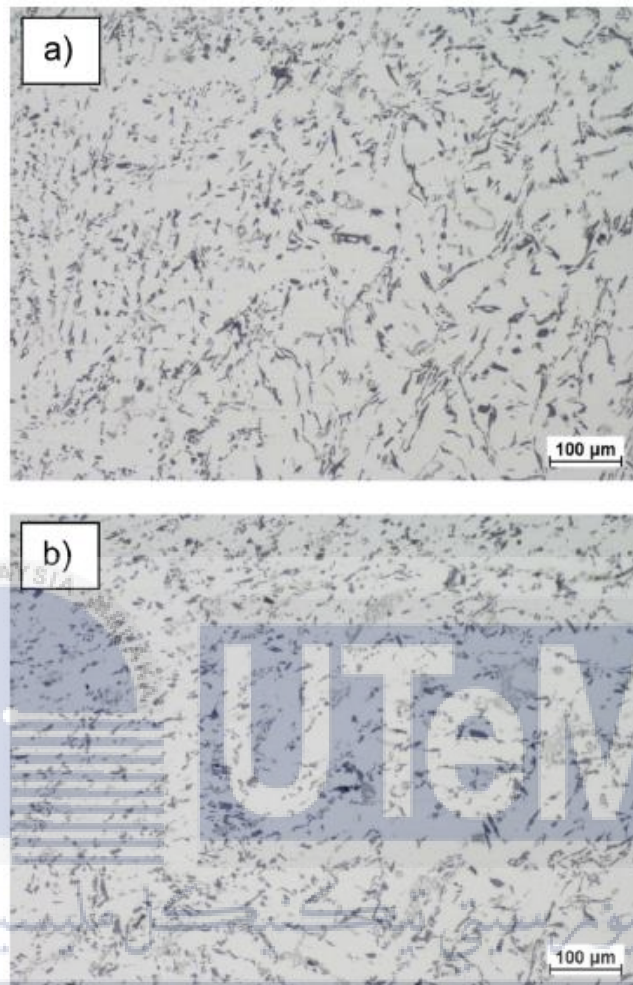


Figure 2.26: Microstructure for retreating side area of (a) FSW welded joint and (b) FSP for, AlSi9Mg (Węglowski, 2018)

Outcome of the experiment shows that advancing side (AS) can be obviously determined for joint welded by using (FSW) process and (FSP). The borders are even for retreating side (RS). The stir zone is observed in above for presence of any dissimilarity. This is because the similar material and parameter of technological, which are for (FSW) welded joint and also for FSP process experience plastic deformation and thermal cycles.

The microstructure of repaired area deals changes crucially with travelling speed and tool rotational speed. As the travelling speed rate becomes slower, it generates high input of heat, therefore it modifies the microstructure, where shows clearly the presence of small grains. Defects joint possess microstructure which is comparable and with big precipitate. During FSP, the heat generated will cause occurrence of plastic deformation and split-up of rough dendrites. Workpiece that experience FSP will undergoes perfection of matrix grains, dissipation of precipitate and shutdown for porosity, thus form a joint that is consistent and free of defects.



2.5 CURRENT WORK IN (FSW) MULTIPASS

A research carried out by Amlan Kar, Satyam Suwas, Satish V. Kailas recently with entitled of “Two-pass Friction Stir Welding of Aluminum alloy to Titanium alloy for improvement in term of mechanical properties”. Two dissimilar metal such as titanium and aluminium used in this research for joining purpose. Welding is done in two pass and the focus of the research is on the outcome of second pass on the deformation and decentralization of Ti, mechanical property of the welded joint and microstructural transformation for Al matrix. In this research, comprehensive characterization carried out for weld joint produced by second pass and the outcome is compared with weld joint produced from first pass in order to study the modification in microstructure following each pass.

Parameter set up for the welding process is tool rotational speed at 800 rpm, traverse speed of 40 mm/min, tool offset of 2.0 mm and plunge depth of 3.5 mm on side of aluminium. To determine the mechanical properties for the joint, tensile test is done. Furthermore, scanning electron microscope (SEM) is utilized for analyzing the microstructure of welded joint. Image from SEM exhibit that joint that has been welded after second pass has high mechanical properties (as from tensile test) as shown in figure 2.27. The welded joint does not have any presence of macro defect and has Ti fragments with variant sizes in excess quantity. The joint also possess high tensile properties. Enlargement image of the micrograph at the interface of joint (area marked by rectangle in red color in figure 2.27 (a)) is displayed by figure 2.27 (b). In figure 2.27 (b), there is a presence of crack which occurred at interface, that cultivate along the marked area in figure 2.27 (b). The crack is formed by interlayer and cultivate within interface zone of Ti. Consequently, it shows that interlayer is main root of cause for crack to occur and ensuing cultivation along the interface that cause occurrence of Ti particles which are dispersed in weld nugget. In figure 2.27 (a), Ti particles can be observed (area marked with circle in green color in figure 2.27 (a)) as shown in figure 2.27 (c). Two types of Ti particles which have dissimilar size can be seen, which is one type particle is bigger than other particle and both particles have cracks and elongated shape.

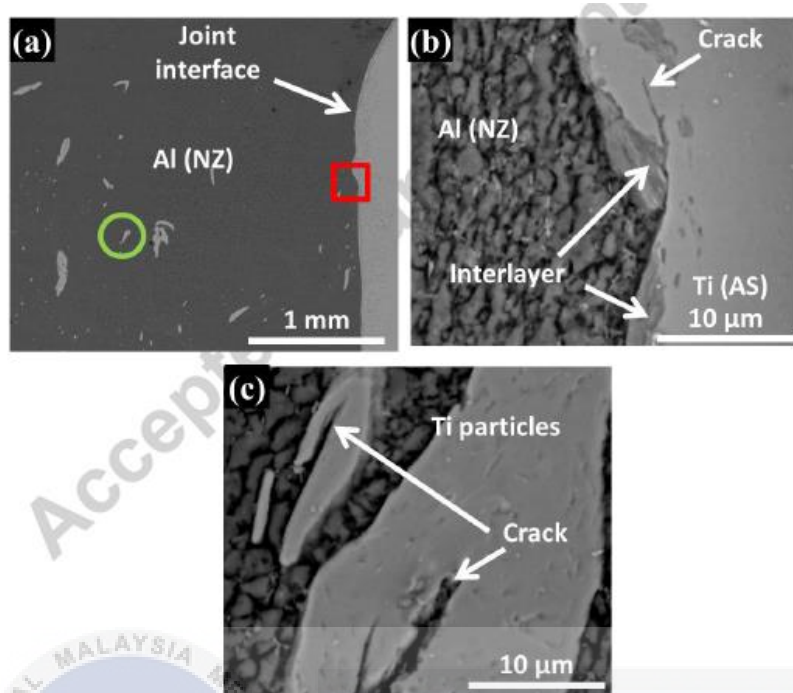


Figure 2.27: Image of (SEM) of the welded joint following second pass of FSW; a) low magnification of SEM micrograph in term of back-scattered electron mode (BSE) of weld nugget exhibits weld, that is free of defects and dispersment of Ti in weld nugget, b) BSE-SEM image from joint interface manifest formation cracks and interlayer, and c) BSE-SEM shows presence image of Ti fragment in weld nugget (Kar, Suwas, & Kailas, 2018)

In order to analyse the mechanical property of a material, microstructural analyse need to be carried out. Electron backscatter diffraction (EBSD) scan is carried out for analyze characteristic of microstructural – crystallographic. The scan performed for first pass and second pass from the middle part of weld nugget. It shows the outcome for first pass. Intermetallic particles and Ti formed as dots, which are in black colour as from lesser indexing value (confident index, $CI < 0.5$). Inverse pole figure (IPF) map shows microstructure at $8\mu\text{m}$ which is very refined. Figure below shows grain boundary character distribution (GBCD). In figure below, detailed examination shows grain located at surrounding of mixed zone (area that consist titanium and intermetallic particles plus aluminum), the area surrounded by black spot that have turned into fully recrystallized (indicated by box in white color). As temperature increases, it will lead to occurrence of static recrystallization (SRX), thus the recrystallized grains is visible around the mixed zone.

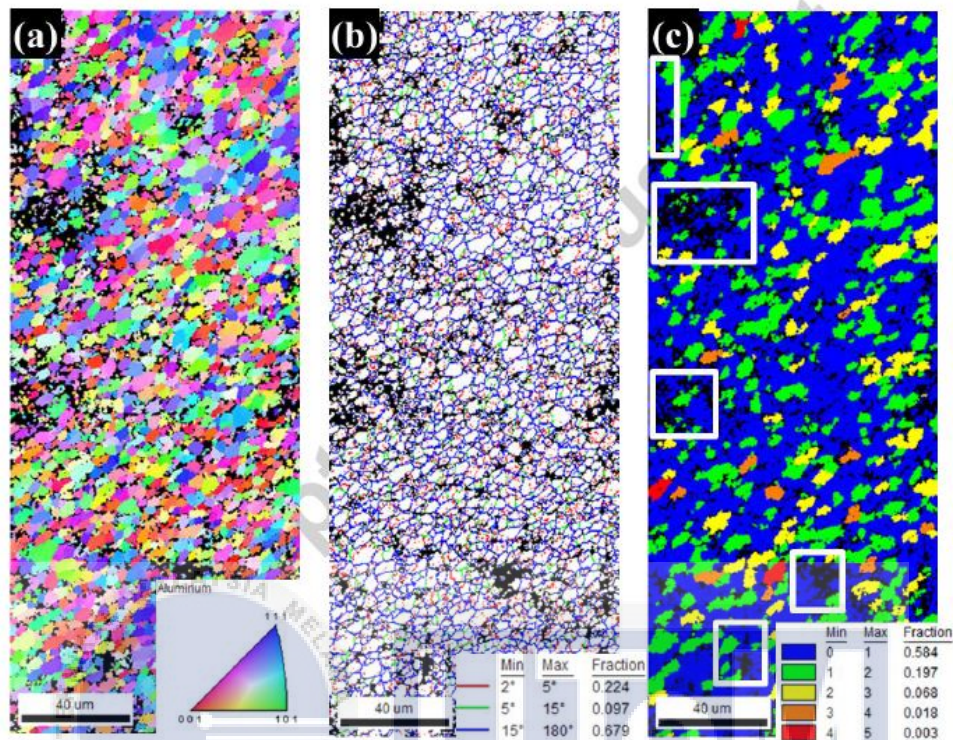


Figure 2.28 : EBSD scan following first pass of Al/Ti FSW and related Orientation Imaging Microscopy (OIM) analysis shows a) IPF with grain boundary map, b) distribution map for grain boundary character and c) Grain Orientation Spread (GOS) map of weld for the middle of the cross-section (Kar et al., 2018)

UNIVERSITI TEKNIKAL MALAYSIA MELAKA

Figure 2.29 below shows microstructural development following second pass by examining EBSD scan. A contingent grain orientation same as first pass but it consists a lesser amount of particles that can be detected by utilizing resolution from EBSD scan in figure 2.29 (a). In figure 2.29 (c), the Ti particles turned into more refined when undergoes second pass, which cannot be detected under EBSD scan. From GOS map in figure 2.29 (c) shows higher amount of recrystallized grains approximately (87%) than first pass from area of weld following second pass.

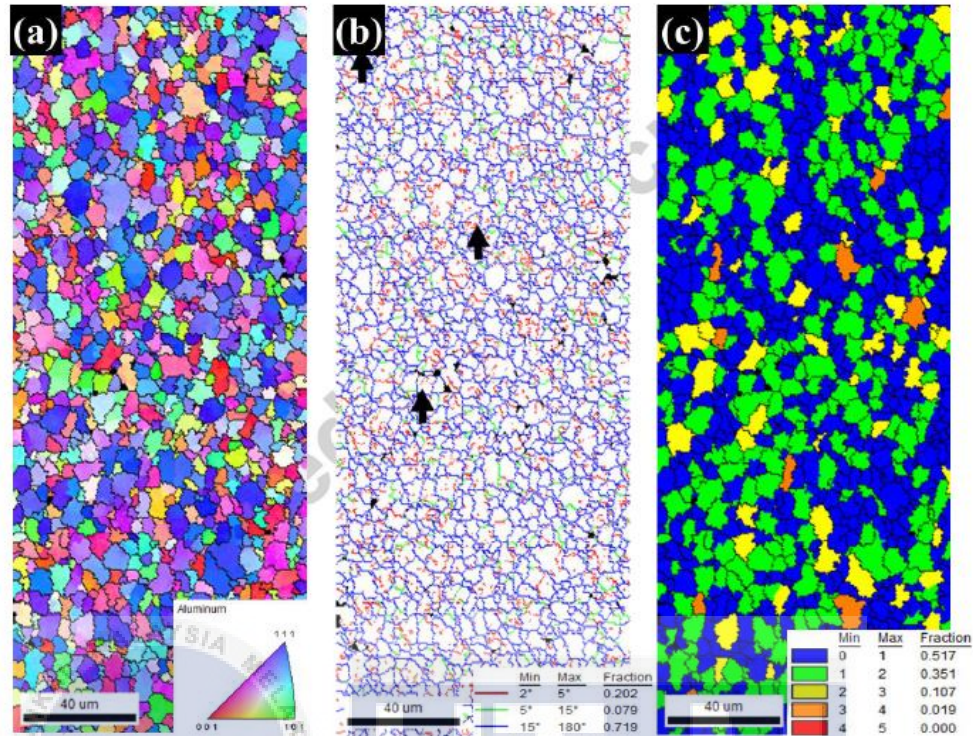


Figure 2.29: Image of EBSD scan following second pass for Al/Ti FSW and OIM analysis shows a) IPF plus grain boundary map, b) distribution map of grain boundary character and c) GOS map of weld of the middle cross-section (Kar et al., 2018)

اونيورسيتي تيكنيكل مليسيا ملاك
UNIVERSITI TEKNIKAL MALAYSIA MELAKA

Ultimate tensile strength (UTS) and ductility test carried out to examine the tensile strength and ductility for sample that undergoes first pass and second pass. Sample that undergoes second pass possess higher tensile strength ((UTS= 271 ± 6 MPa) and ductility of (9 ± 1.0 %) in contrast with sample that undergoes first pass with tensile strength of (231 ± 8 MPa and ductility of 7.4 ± 0.3 %). Joint efficiency used to define the quality of welded joint. It will be calculated as ratio of Ultimate tensile strength (UTS) of the weld produced to (UTS) of the base material. As in the investigation, joint efficiency for first pass is 50 % and for second pass is 60 %.

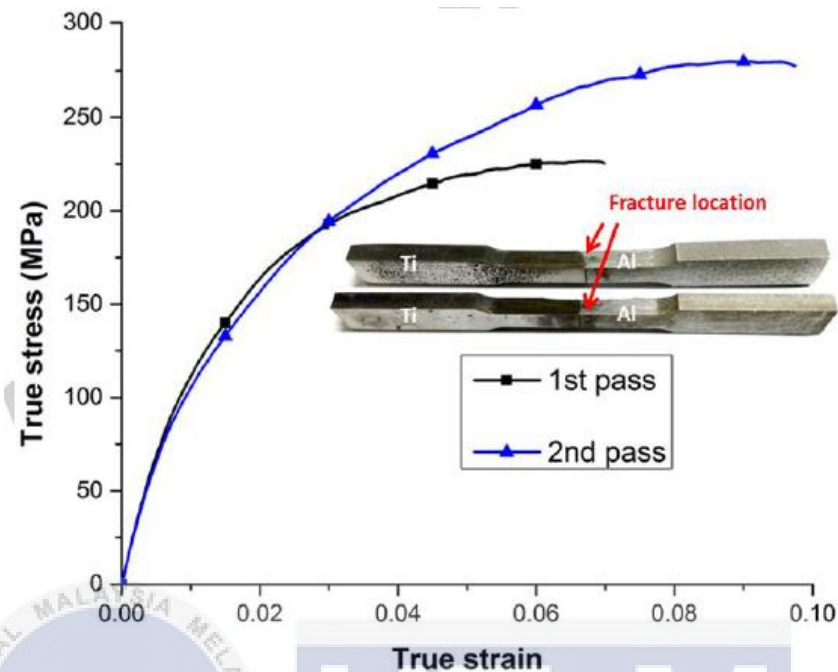


Figure 2.30: Graph above shows True stress vs. true strain plot for the welds at produced different pass of the weld revealing a difference in term of tensile strength and ductility, the highest tensile property being shown of the weld after second pass (Kar et al., 2018).

Analysis of outcome for second pass towards modification of microstructure done in this study. Joint weld that undergoes second pass has higher amount of recrystallized grains about 87% when compared with first pass that have about 78%. This is because when the workpiece experience second pass, it will be exposed towards higher heat. Occurrence of drastic deformation that disseminate strain heterogeneous across cross section of the welded joint that causes generation of evaluated residual stress. It leads to further transformation of recrystallized grains, which located in the nugget zone.

Workpiece that subjected to second pass encountered growth of grain in the weld nugget as it got higher input of heat compared with first pass. In figure 2.31 (b), modification of large amount of recrystallized grains causes higher in the misorientation angle distribution (MAD) that leads to increase in amount of recrystallized grains after second pass. This feature leads to

evolution of high amount of recrystallized grains across the method of static recrystallization (SRX), Dynamic Recovery (DRV) and Continuous Dynamic Recrystallization (CDRX).

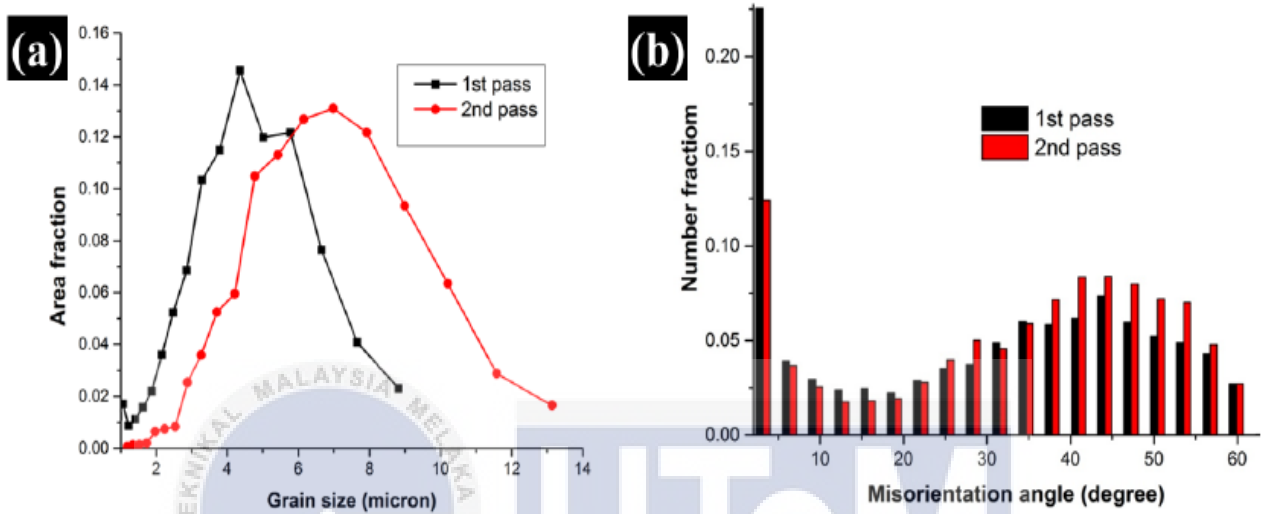
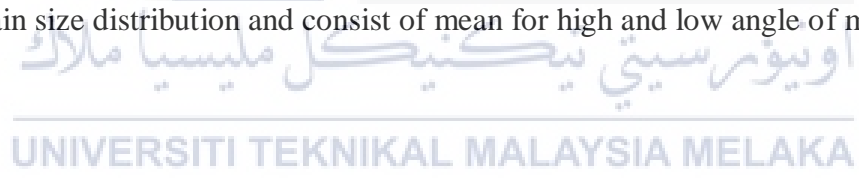


Figure 2.31: Comparison done in graph form for a) distribution of grain size b) misorientation angle distribution of welds for first and second pass with optimized process variable that shows Gaussian grain size distribution and consist of mean for high and low angle of misorientation.



Another study conducted by (Xu, Ueji, & Fujii, 2015) with title of “Improved mechanical properties for 70/30 brass joint by multi-pass friction stir welding with rapid cooling”. The experimentation done by using friction stir welding process with a load controlled machine. Workpiece used in this experiment is cold rolled commercial 70/30 brass plates. The process was done by utilizing argon gas flowing constantly surrounding the rotating tool at flow rate of 20 L min^{-1} to avoid occurrence of oxidation at stir zone (SZ). Rapid cooling done by exposing the workpiece with directing liquid CO_2 ($-78 \text{ }^\circ\text{C}$). Field emission scanning electron microscope (FE-SEM) used for conducting measurement of Electron backscatter diffraction (EBSD). By operating transmission electronic microscopy (TEM), substructures located in the stir zone were categorized.

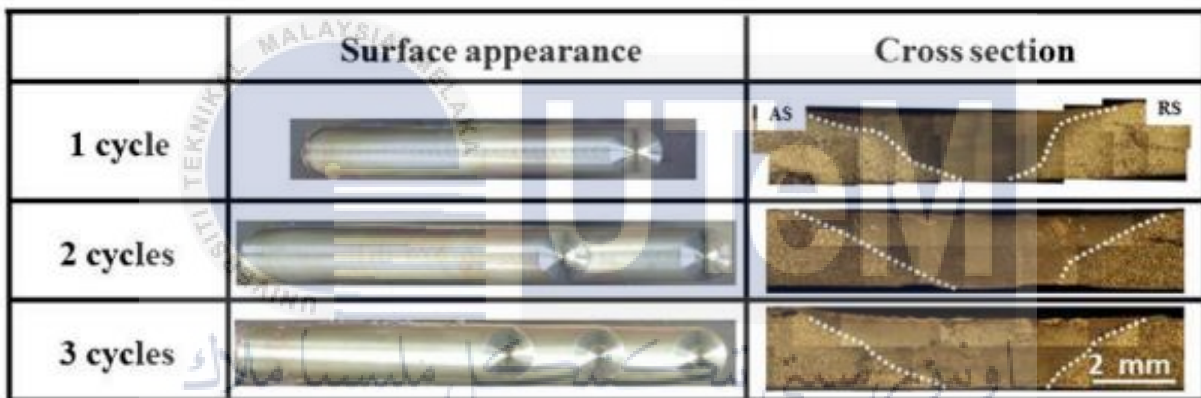


Figure 2.32: Surface appearance and cross section of weld produced with number of cycles respectively in macroscopic view : AS - advancing side and RS - retreating side (Xu et al., 2015)

From the figure above, it can be observed that the weld produced is free from defects and oxidation was not formed as effect of using shielding gas and improved cooling rate. The macroscopic view revealed that there was no presence of defects at internal portion of weld. As the number of cycles increases, it causes area of stir zone (SZ) becomes larger. It occurred so because of elevation of plastic strain.

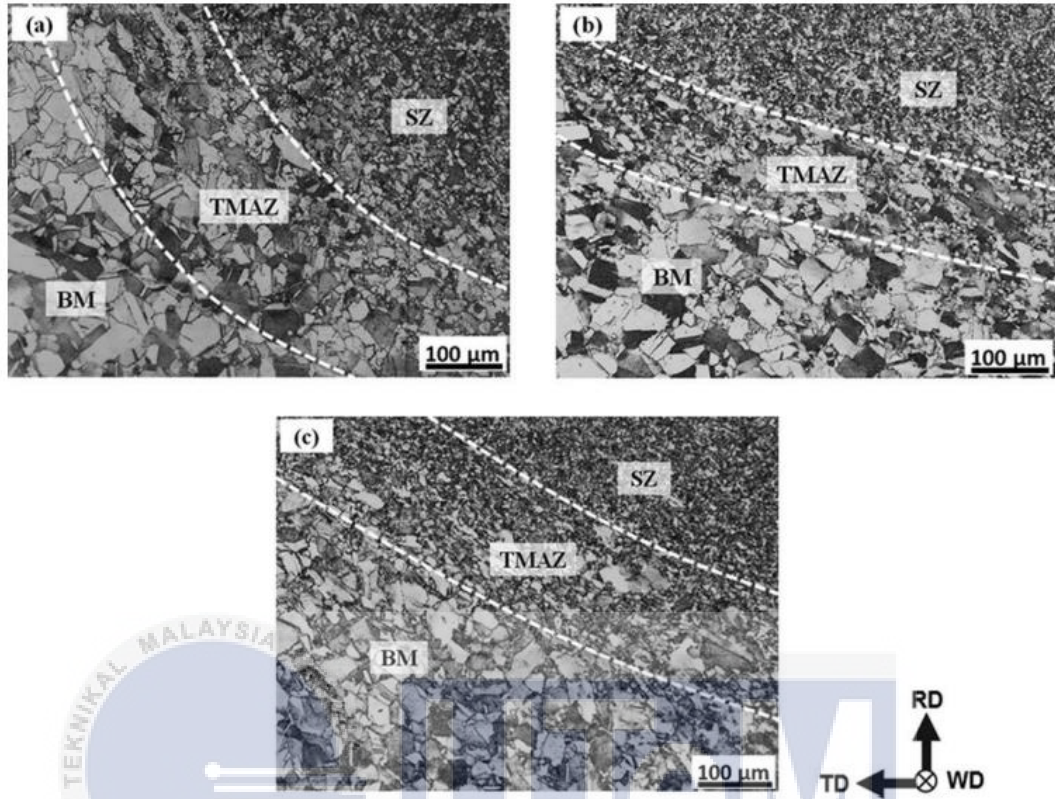


Figure 2.33: Microstructures of advancing sides for the joints welded by (a) 1 cycle, (b) 2 cycles and (c) 3 cycles (Xu et al., 2015)

Figure above shows the view of microstructure of stir zone (SZ), which is placed in the advancing side (AS) for each joint produced. Based on past research done for FSW process, two different areas such as (HAZ) between the TMAZ and the base metal and (TMAZ) around the (SZ) will be portrayed by the microstructure located at transition between base metal and (SZ) (Xu et al., 2015). (HAZ) will not be identified in joint made from FSW process from any cycles because of swift heat distribution by extra liquid cooling, which is CO₂. There was presence of grains of TMAZ that is deformed and elongated pattern surrounding the (SZ).

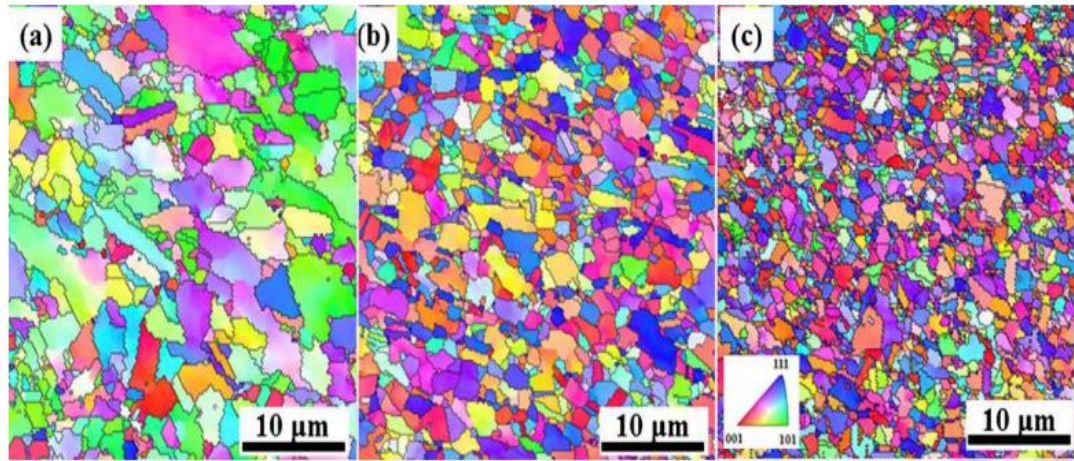


Figure 2.34: Orientation of colour maps of centre SZ for (a) 1 cycle, (b) 2 cycles and (c) 3 cycles (Xu et al., 2015)

Microstructure for 1 cycle is in heterogeneous and have small sized grain ($0.5\mu\text{m}$) and also in large sized ($9\mu\text{m}$) as it did not get sufficient plastic strain for accomplished grain refinement. In 2 cycle, SZ shows comparable similarity in grain structure when in contrast with 1 cycle. It has mean size of grain about $2.6\mu\text{m}$. As the number of cycles elevated to 3, SZ possessed grains which were more constant grains and much refined. The mean size of grain for SZ was refined to $0.8\mu\text{m}$. When the cycle is increased for FSW process, it causes the weld to have high ultimate tensile strength, yield strength and hardness. The experiment proved that increasing cycle number will lead good ductility property of weld produced and benefit of multipass for FSW process.

2.6 METALLURGICAL WORK FOR GRAIN STRUCTURE

Metallurgy can be defined as study of metallic property of a matter in order to obtain benefits from metals in our life. Generally, metallurgical work is focused on analyze of microstructure for the metal elements. In research carried out by (Derazkola, Aval, & Elyasi, 2015), the samples that used is AA1100 and it had been welded were cut according to desired length from the joint produced that consist of stir zone (SZ). Firstly, the samples underwent grinding process emery paper or also known as abrasive paper of different grades. Then, disc polishing machine used as end polishing by implement diamond compound. The samples were later etched with 10% Sodium Hydroxide (NaOH) as it helps to get pattern of flow in the alloy. Light microscope is used to get a clearer view of the microstructure. Furthermore, scanning electron microscopy (SEM) and X-ray diffraction (XRD) method used for examining the generation of intermetallic compound at areas that underwent welding process. Moreover, the examination for strength of weldness was also carried out. The samples were prepared based on American Society for Testing and Materials (ASTM). Shimadzu Vickers indenter used for determine the hardness of the welded joint by using a test load of 0.2 kgf for 15 s. In addition, tensile test also performed on the samples by utilizing crosshead speed of 1 mm/ min^{-1} .

UNIVERSITI TEKNIKAL MALAYSIA MELAKA

2.7 CONCLUSION

Table 2.8: Previous works regarding multipass

AUTHOR	TOPIC	TYPES OF FSW USED	OUTCOME
Amlan Kar, Satyam Suwas, Satish V. Kailas	Two-pass Friction Stir Welding of Aluminum alloy to Titanium alloy: A Simultaneous Improvement in Mechanical Properties	Conventional friction stir welding	Weld joint after second pass exhibit higher tensile strength compared with one pass due occurrence of recrystallization of grains in second pass. Furthermore, defect free joint is obtained after second pass.
N. Xu*, R. Ueji and H. Fujii	Enhanced mechanical properties of 70/30 brass joint by multi-pass friction stir welding with rapid cooling	Conventional friction stir welding with rapid cooling.	As number of cycle increase, the grains were further refined that enhanced the tensile strength of the sample. Total of three cycles were performed. As the number of cycle increase, the tensile strength also increased.
Ravinder Singh ¹ , Inderjeet Singh ² , Gagandeep Singh Sandhu ³ , Farman Khan ⁴ , Jagjeet Singh	Mechanical and Metallurgical Properties of Multipass Friction Stir Welded Joints of Aluminium 6061 Alloy Microstructure and fracture toughness of multipass friction stir welded joints of API-5L-X80 steel plates	Conventional friction stir welding	Highest tensile strength contributed by two pass of AA 6061. Research able to produce joints that is free of defects aluminum alloy 6061. The multipass of weld joint is affected by tool rotational speed and profile of tool pin

Julian A. Avila a,b,n, Johnatan Rodriguez a, Paulo Roberto Mei b, Antonio J. Ramirez	Microstructure and fracture toughness of multipass friction stir welded joints of API-5L-X80 steel plates	Conventional friction stir welding	As number of pass increase, there is increase in term of fracture toughness for the sample. The microstructure of the joint contains bainite packets M-A (martensiteaustenite) that situated inside boundary packets between plates at two pass.
C. Leitao , E. Arruti b, E. Aldanondo b	Aluminium-steel lap joining by multipass friction stir welding	Conventional friction stir welding	Three pass has no presence of intermetallic at interface of Al-Fe. Three pass produce highest hardness compared with one pass and two pass.

Previous studies mostly used conventional frictional stir welding for multipass and there is no research carried out by multipass of bobbin friction stir welding. Thus, this research is conducted.

This chapter discussed about previous studies that carried out for multipass of friction stir welding (FSW) by using similar metals and dissimilar metals and its effects on microstructure of the welded joint. Multipass welding is an effective method to repair joint and for producing joint that has high strength by refining the grains. However, parameter set up for FSW process is crucial and need to be considered in order to produce joint that is free of defects. Scanning electron microscope (SEM) and Optical microscope (OM) are generally implemented to analyze the microstructure of samples.

CHAPTER 3

METHODOLOGY

3.0 INTRODUCTION

This chapter provide specified details for organization and technique for conducting the experiment to attain the objective of the study. Multipass of Bobbin friction stir welding (BFSW) is done for joining aluminum alloy 1100. In this chapter, all the techniques that used for this research is explained gradually. This chapter also present comprehensive guideline instruction for the experiment conducted right from beginning to the end. Comprehensive preparation for this chapter consists of preparation of material and welding parameter setup (number passes).

Analyze done by utilizing mechanical test for the weld produced and observation carried out on microstructural evolution for fulfilling objectives for this research. In the next section, data obtained from methodology is shown.

3.1 FLOWCHART OF PROCESS

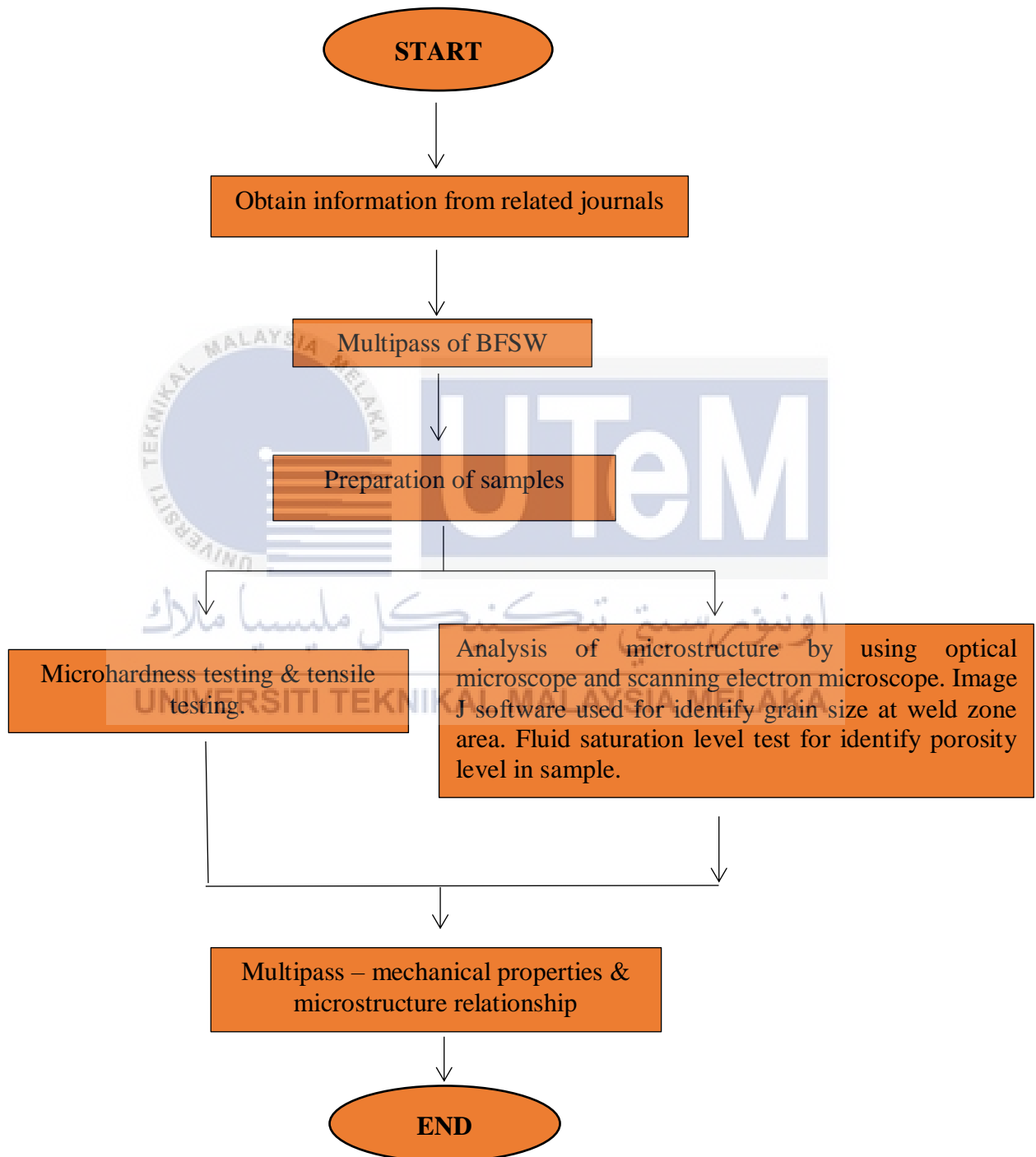


Figure 3.1: Flowchart for BFSW process

3.2 PARAMETER SETUP FOR MULTIPASS BFSW

The objective of current study is to analyze the effect of multipass BFSW on microstructure of AA1100. The operation of BFSW is run for one pass, two pass and three pass.

Table 2.9: Parameter setup for the experiment

Parameters setup	Settings done
Number of pass	One pass, two pass & three pass
Tool rotation (rpm)	900
Traverse speed (mm/min)	One pass- 105 , two pass -155 & three pass - 205

3.2.1 PREPARATION OF WORKPIECE FOR EXPERIMENT

The material used for the study is AA1100. The aluminum plate with thickness of 6mm is used for welding. Initially, the AA1100 plate is cut into dimension of 140 mm (as for length) x 120 mm (as for width) by utilizing shearing machine.

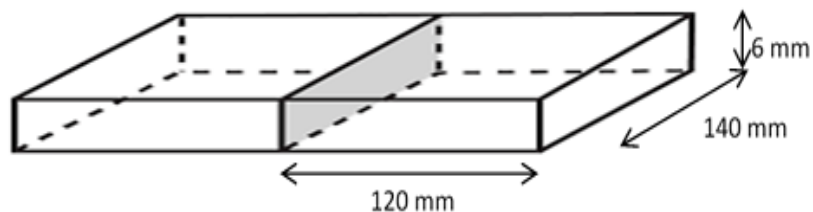


Figure 3.2: Dimension of workpiece

Then, drilling of two holes with diameter of 15 mm is done at gap of 60 mm which is parallel from the joint. To reduce the effect of vibration at entry of tool, the workpiece needs to be fixed at center.

3.2.2 TYPE OF BOBBIN TOOL USED

H13 tool steel rod with diameter of 50 mm is used for the experiment conducted as bobbin tool for BFSW. Dimension of tool is

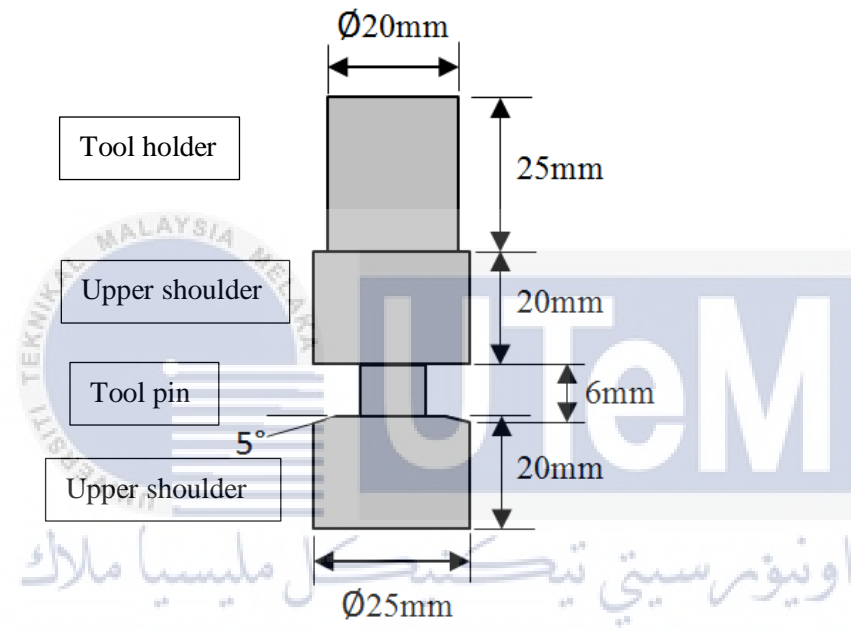


Figure 3.3: Dimension of tool

3.2.3 EXPERIMENT SETUP

Machine used for the multipass BFSW is computer numerical control (CNC) lathe machine model HAAS VOP-C.

3.2.4 SETUP FOR BFSW WELDING

The joint of need to be parallel to the direction of welding. The screw needs to be ensure well tightened in order for safety purposes.

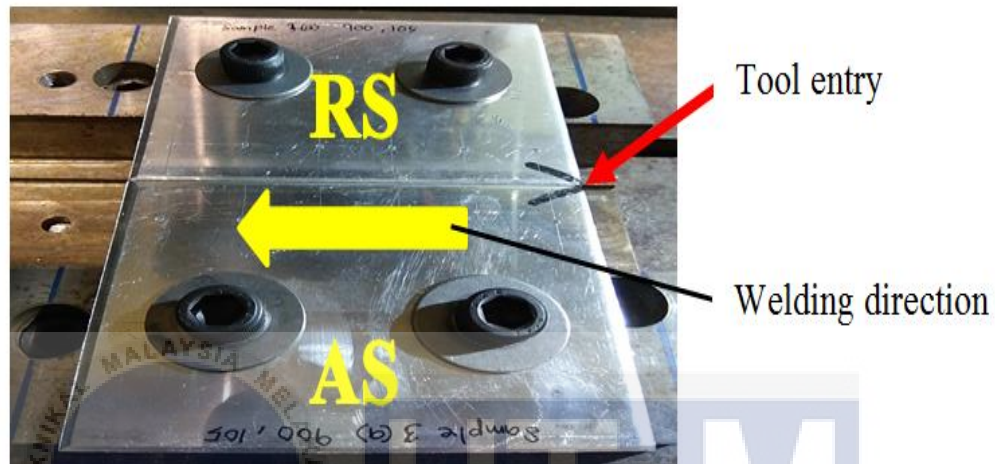


Figure 3.4: Plates in butt joint

Once the plates are fixed tightly, the CNC machine is programmed for the tool to starts precisely at middle of entrance. The welding process is done for one pass then two passes and followed by three passes. The aluminium plate is allowed to cool down at room temperature. This strategy utilized to remove the impact of heat that is gathered for two passes and three passes at end of each pass. After that, the welding process done subsequently for pass.

3.3 SAMPLE PREPARATION

AA1100 plate is cut by using by using bandsaw machine into rectangular shape with dimension of (4.4 cm x 1.3cm) that has thickness of 0.6 cm onto 3 pieces of samples. Bandsaw machine is chosen for cutting process rather than laser cutting process as it induces least heat affected zone (HAZ). Laser cutting process will cause the workpiece to be heated thus causing modification in microstructure that can affect the accuracy of result obtained.

3.4 MICROHARDNESS TESTING

Analysis for hardness of weld joint produced from multipass is tested by using microhardness machine. Load of 0.2kgf used on samples during indentation for 15 seconds. Figure 3.5 below shows the analysis for hardness mapping. The hardness of sample is tested at three different part of sample, which are top, center and bottom to get an accurate data for analysis. Total of 45 indentation diamond done on every sample with a distance of 1 mm between each indentation for top, center and bottom level.



Figure 3.5: Hardness mapping for sample



Figure 3.6: Microhardness Tester machine

3.5 OPTICAL MICROSCOPE (OM)

Optical microscope (OM) used for analyzing shape and size of grains for the samples. For observing under OM and SEM microscope, samples undergo few steps:

- A. Grind the samples by using paper silicon carbide at level of 200, 400, 600, 800 and 1200.
- B. Samples undergoes polishing process by using polishing pad and diamond slurry with range of 6 μm , 3 μm and 1 μm .
- C. The polished samples need to etch with chemical solution, keller reagent to get clearer view on microstructure for samples.



Figure 3.7: Optical Microscope

3.6 SCANNING ELECTRON MICROSCOPE

Scanning electron microscope (SEM) used for analyzing changes in microstructural and also to detect presence of any defects in detailed manner.



Figure 3.8: Scanning electron microscope (SEM)

3.7 GRAIN SIZE MEASUREMENT

In order to identify size of grain for each sample after obtained image of SEM, software known as ImageJ is used.

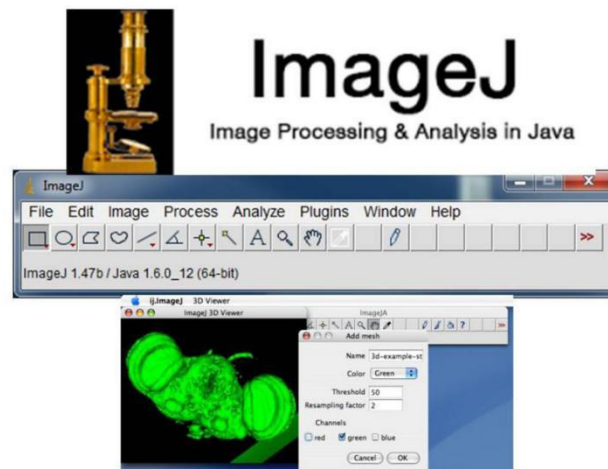
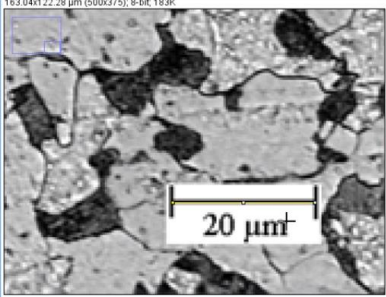
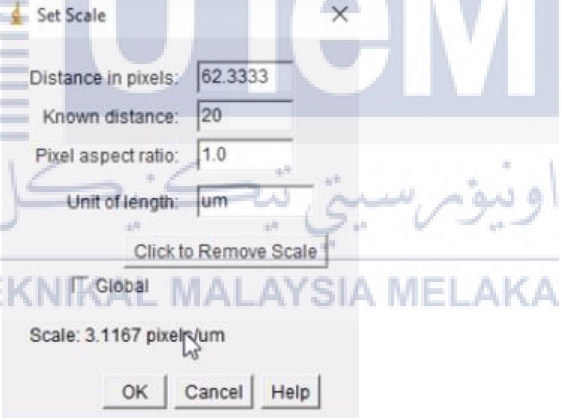
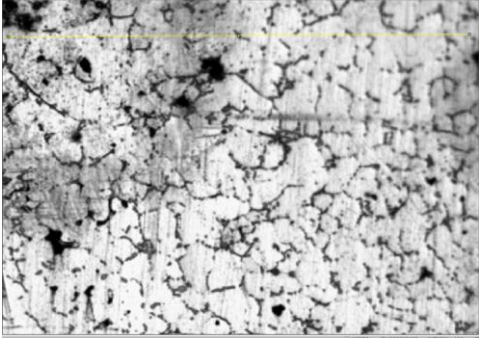
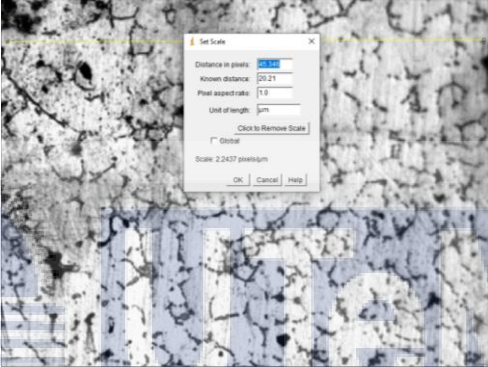


Figure 3.9: ImageJ software

Few steps need to be carry out to in order to obtain average grain size in ImageJ software.

Table 3.1: Steps to calculate average grain size




1.	 <p>Figure 3.10 : Line matching according scale line</p> <ul style="list-style-type: none"> • Draw a line matching according to the scale line.
2.	 <p>Figure 3.11 : Information display regarding the scale</p> <ul style="list-style-type: none"> • Key in scale of image in second column and also unit of the image.

3.	 <p style="text-align: center;">Figure 3.12 : A long yellow line drawn</p> <ul style="list-style-type: none"> • Draw a long line on the image.
4.	 <p style="text-align: center;">Figure 3.13 : Display of information regarding the length of yellow line drawn</p> <ul style="list-style-type: none"> • Click on icon that displays “analyse” and click the option showing “set scale”.
5.	<ul style="list-style-type: none"> • Manually count the number of grains that located on top of the yellow line.
6.	<p style="text-align: center;">Average Grain Size (Line Intercept Method)</p> $\text{Average Grain Size} = \frac{\text{Line Length}}{\text{Number of Grains}}$ <p style="text-align: center;">Figure 3.14 : Formulae to calculate the average grain size</p> <ul style="list-style-type: none"> • By using formulae above, we need to key in the details for the line length. Details of line length can be obtained from the known distance as shown in step 4.

3.8 ANALYSIS FOR POROSITY LEVEL IN SAMPLE

In order to obtain the level of porosity in sample welded by one pass, two pass and three pass by using fluid saturation level that works by principle of Archimedes.

Table 3.2: Steps that need to be performed for fluid saturation level test

1	 <p>Figure 3.15 : Electronic scale</p> <ul style="list-style-type: none"> • Measure initial mass of sample by using electronic scale.
2	 <p>Figure 3.16 : Water filled inside beaker</p> <ul style="list-style-type: none"> • Fill water in beaker for about 30ml of water and placed on electronic scale to get the mass. Density of water is calculated by dividing the mass of water with volume of water. Density of water - 0.99987 g/cm^3
3	<ul style="list-style-type: none"> • Dip the sample in water for about 2 minutes and stopwatch is used for recording time taken.
4	 <p>Figure 3.17 : Sample placed on tissue cloth</p> <ul style="list-style-type: none"> • Roll the surface of sample on tissue cloth to remove any excess water droplet that may affect the reading accuracy before taking its mass.

5	<ul style="list-style-type: none"> Measure the mass of sample and repeat the step for 3 times for obtaining average mass for improving accuracy of reading.
6	<ul style="list-style-type: none"> The difference in mass of sample is then divided with the density of water.

3.9 ULTIMATE TENSILE TESTING

Tensile testing was performed by utilizing universal testing machine. Type of model of machine used is known as INSTRON-5969. Table 3.3 below shows machine specifications.

Table 3.3: Machine specification of tensile testing machine

Method of measured and display	Digital display
Maximum Load	50kN

In order to analyze the tensile strength, the sample should be cut according to specified length and shape. To get the cross-section of welded joint, the samples were cut perpendicularly. By using CNC five-axis milling machine, the samples were cut according ASTM E8/E8M as shown in figure below. Two samples were prepared for each consequent number pass for tensile testing purposes.

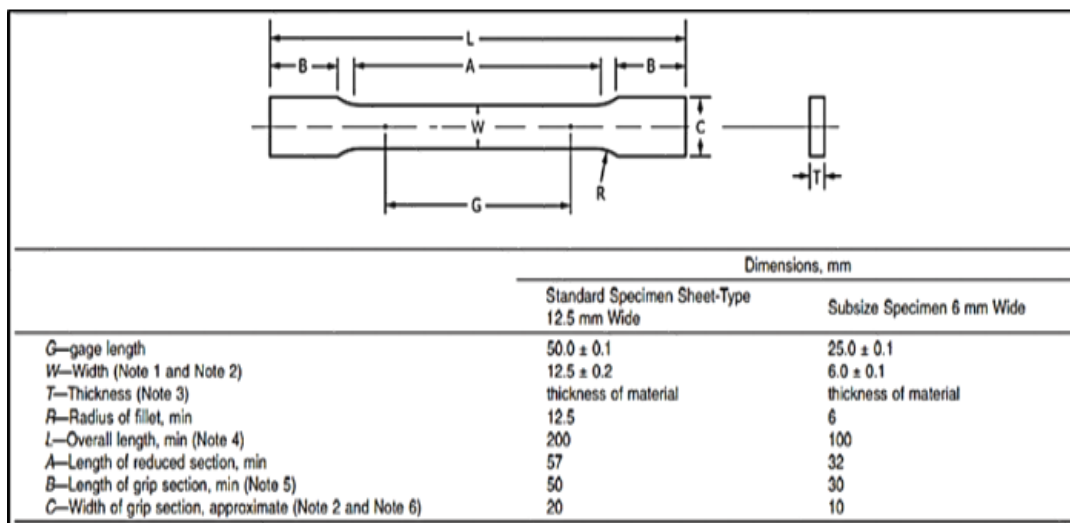


Figure 3.18: Drawing of ASTM E8/E8M standard for tensile testing

CHAPTER 4

RESULT AND DISCUSSION

In this chapter 4, the outcome from multipass of bobbin friction stir welding on aluminium alloy 1100 will be analyzed. Optical microscope and scanning electron microscope (SEM) are utilized for examining microstructure evolution at weld zone for the samples. Fluid saturation level test done for identifying porosity level in samples. Microhardness tester machine used to examine hardness property and ultimate tensile strength test used for analyzing tensile strength of the AA1100 samples.

4.1 VISUAL INSPECTION OF WELDED JOINT

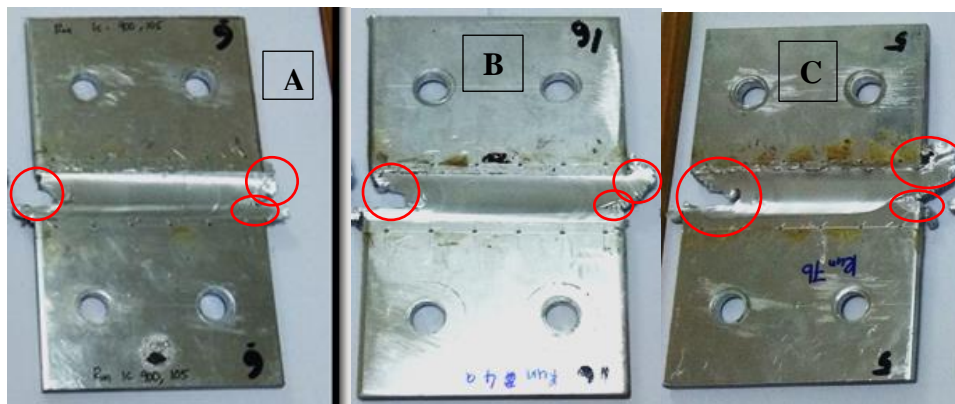



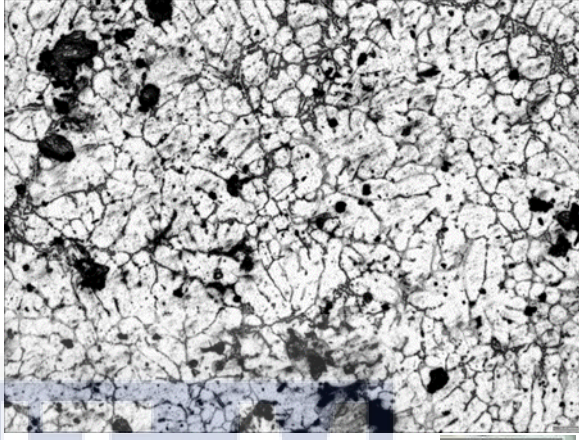

Figure 4.1: Welded sample A) One pass B) Two pass C) Three pass

Figure 4.1 shows the welded samples for one pass, two pass and three pass. However, there can observed presence of flash, incomplete weld and formation of tunnel. All the defects are indicated by red circle. As for sample welded by three pass, the joining process is incomplete. The parameter of welding such too rotational speed kept constant throughout the welding process, which is 900 rpm. Travel speed of bobbin tool is set at different speed. For this welding process, parameter of the machine such welding speed (mm/min) set at 105 (mm/min) for one pass, 155 (mm/min) for two pass and 205 (mm/min) for three pass. The presence of flash is smaller in one pass. As the number of pass is increased, the size of flash also increased.

4.2 MICROSTRUCTURAL OBSERVATION UNDER OPTICAL MICROSCOPE

Microstructural observation is crucial in order to identify the property of a material. The microstructure at weld zone area examined for each sample. Optical microscope used to obtain a clearer image to identify grains size for one pass, two pass and three pass. Comprehensive characterization was done for the weld corresponding with second and three pass and also the outcomes were compared with sample welded by one pass to identify the changes occurred in microstructure following each pass.

Table 4.1: OM image at weld zone area with average grain size for a) one pass (3.87 μm), b) two pass (2.54 μm) and c) three pass (3.22 μm) at magnification of 10X.

a) One pass	b) Two pass
 <p data-bbox="240 947 350 982">3.87 μm</p>	 <p data-bbox="850 947 961 982">2.54 μm</p>
<p data-bbox="760 1079 948 1115">c) Three pass</p>  <p data-bbox="483 1654 594 1690">3.22 μm</p>	

Based on the table above, the average grain size of sample that underwent two pass exhibit the smallest size when compared with one pass and three pass. Grains in one pass slightly elongated in contrast with grains in three pass. The initial grain size after one pass was 3.87 μm . When number of pass is increased from one to two pass, there was decreased in average grain size at weld zone area from 3.87 μm to 2.54 μm . As number of pass is set at three pass, average grain size increased from 2.54 μm to 3.22 μm . The main factor that influenced average grain size is the rate of heat input. During bobbin friction stir welding process, rotational action of bobbin tool produced heat due to friction that altered the microstructure at weld zone area. Formation of weld zone in BFSW is caused by dynamic recrystallization. Microstructure at weld zone for second pass shows smaller average grain size in contrast with one pass as the grains have been recrystallized. As the number of pass increased from one to two pass, the sample experienced higher heat than one pass due to continuous stirring process by two times from bobbin tool in second pass during joining process. Thus, it caused further modification in recrystallization of grain at the weld zone area. Sample welded by two pass consist of more grains fragment that were recrystallized in contrast with one pass. In two pass, uniformity of dynamic recrystallization is exhibited by the AA1100. Dynamic recrystallization led to refining of microstructure for two pass. Continuous stirring action of bobbin tool promoted additional dynamic recrystallization in two pass when compared with one pass. According (Xu, Luo, & Fu, 2018), the frictional heat and strain level of plastic deformation that included with level of recrystallization affect the difference in average grain size. Microstructure at weld zone area for two pass exhibited fine equiaxed of recrystallized grains than one pass.

When number of pass was elevated from two to three pass, it resulted increase in average grain size. The average grain size in three pass is smaller when compared with one pass. In three pass, sample exposed to a very high elevation of heat and intense plastic deformation that resulted in prominent growth of grain which caused formation of coarse grains that is inhomogeneous. It is believed that high heat energy caused region of HAZ for the joint to be extended and HAZ is advanced further from weld zone by the input of heat energy. Grains that located near the weld zone enlarged when subjected to higher heat. Coarse grain occurred in three pass due to rise in temperature as the high heat influenced the declination of cooling rate. (Kowser & Motalleb, 2015) states that cooling rate gives impact to the size of grains and the

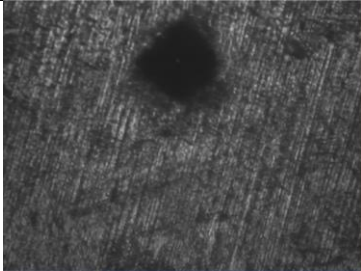
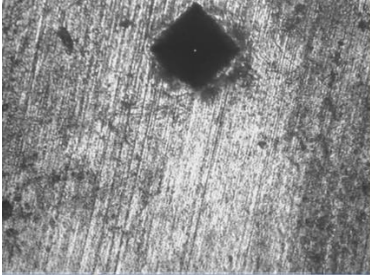
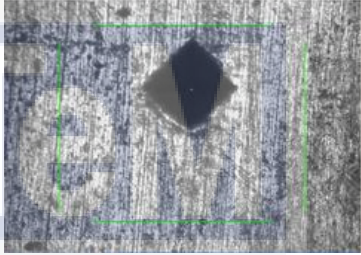

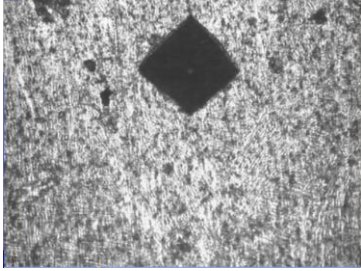
mechanical property and also mechanical property will be enhanced when metal exposed to higher rate of cooling upon heating at high temperature.

4.3 MICROHARDNESS TEST RESULT

During microhardness testing process, indentation done from retreating side (RS) to advancing side (AS). Microhardness profile across the welded area of sample will be different along the depth. Hence, microhardness profile measured at three dissimilar depth level, which are top, centre and bottom to obtain the most precise results. The hardness of base metal before weld is 47 HV. Total of 45 indentation diamond done on every sample with a distance of 1 mm between each indentation. Strain force will be formed if the indentation done nearer with another indentation, thus it will influence the accuracy of hardness result. For each sample, test load is set at 0.2 kgf for 15 seconds. Hardness test done on three parts of same surface for every sample, which are top, centre and bottom in horizontal direction. From observation, the graph of microhardness for top, centre and bottom shows W-shape curve as a result of elevation in plastic strain at specified regions. The higher the value of HV, the higher the hardness.

UNIVERSITI TEKNIKAL MALAYSIA MELAKA

Table 4.2: Indentation at each zone for One Pass

<ul style="list-style-type: none"> • Base Metal, RS 	
<ul style="list-style-type: none"> • Heat Affected Zone, RS 	
<ul style="list-style-type: none"> • Thermo-mechanically Affected Zone, RS 	
<ul style="list-style-type: none"> • Weld Zone 	
<ul style="list-style-type: none"> • Thermo-mechanically Affected Zone, AS 	

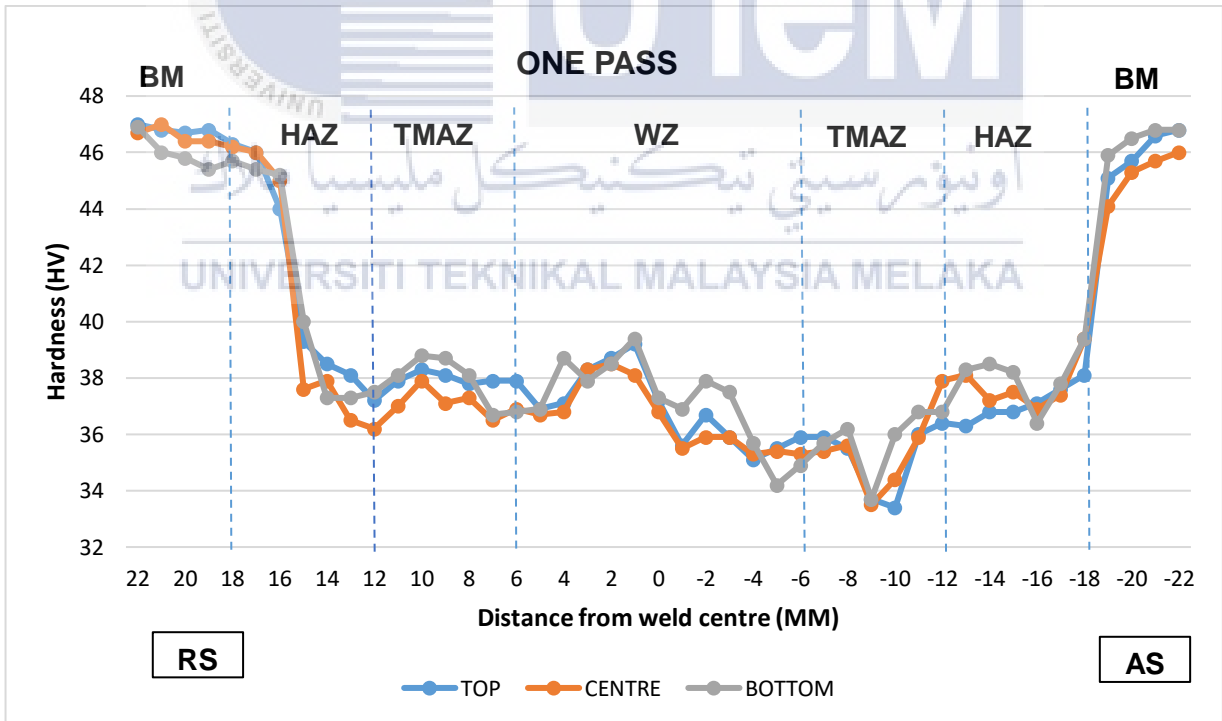
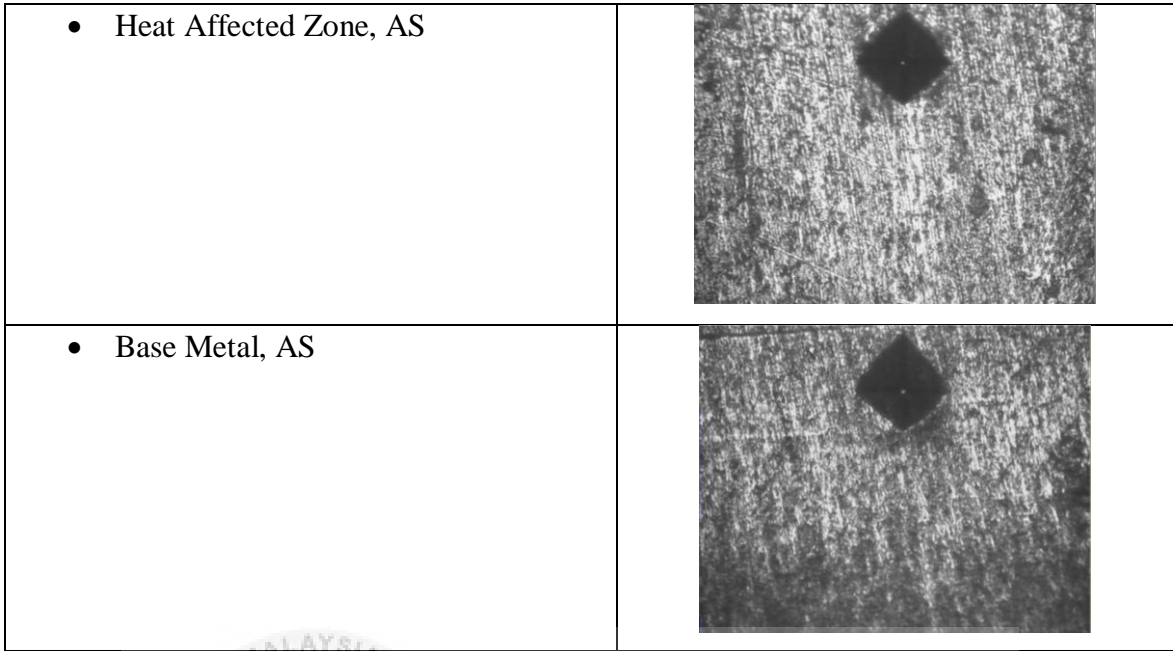
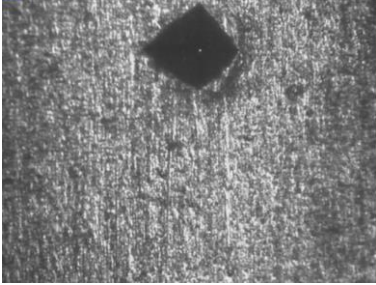
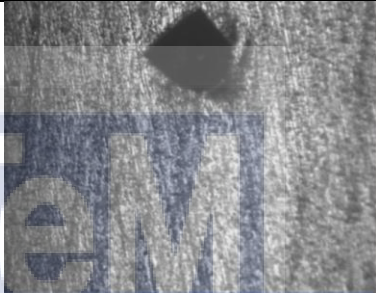


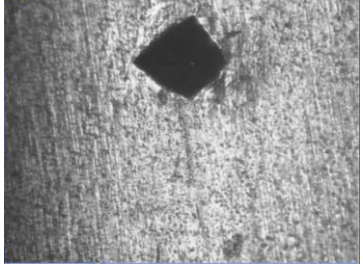
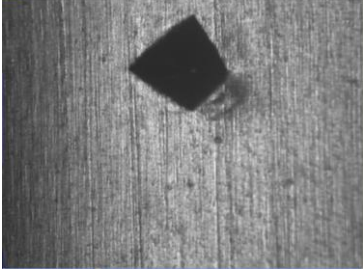
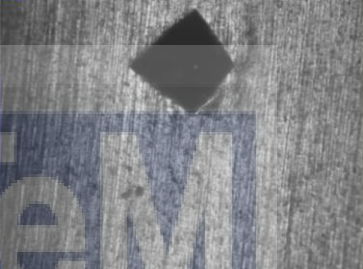

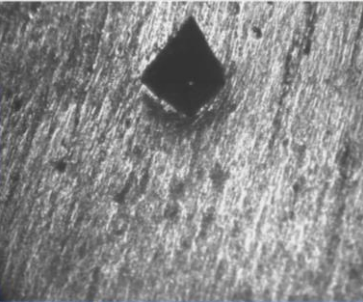
Figure 4.2: Microhardness graph for one pass

From figure 4.1, hardness at retreating side (RS) is higher than advancing side (AS) as bobbin tool rotates from (AS) to (RS), it stirred material from AS to RS region. The initial diamond indentation point at top produce value of 47 HV, centre is 46.7 HV and for bottom is 46.9 HV. At region from 16 mm to 15 mm from weld centre, hardness value decreases drastically for top, centre and bottom parts. Hardness value decrease from 44 HV to 39.3 HV for top part about 10.7%. For centre part, hardness reduced from 45 HV to 37.6 HV for centre part about 16.4%. As for bottom part, hardness decreases about 11.5% when reduced from 45.2 HV to 40 HV. Hardness of the area that known as heat affected zone (HAZ) declined as result of heat energy during BFSW process. Heat energy from BFSW causes separation of fine precipitation at welded joint area. Dissolution and coarsening of the precipitates from region of heat affected zone to stir zone caused the hardness drop sharply from the graph pattern. When the area of weld exposed to heat energy, it resulted increase in size of precipitate that altered the mechanical properties in term of hardness for the sample to be softer than the base metal. Grains of base metal that is located further away from weld area recrystallize into smaller shape that resulted in higher value of hardness at base metal. Decrease in value of hardness for RS and advancing side AS is nearly similar. At region from -18 mm to -19 mm from weld centre of AS, value of hardness increases tremendously for all three part of sample. The increase in hardness for top level is from 38.1 HV to 45.1 HV about 18.4% and for centre level is from 39.4 HV to 44.1 HV with percentage of 11.9%. As for bottom, value of hardness escalates from 39.4 HV to 45.9 HV about 16.5%.

As for each zone, hardness range for base metal (BM) of retreating side (RS) is 45.4 HV - 47 HV and for heat affected zone (HAZ) of RS is 36.5 HV – 46 HV. Range of hardness in thermo-mechanically affected zone (TMAZ) at RS is 36.7 HV – 38.8 HV and for weld zone (WZ) is 34.4 HV – 39.4 HV. Furthermore, hardness range at TMAZ for advancing side (AS) is 33.4 HV – 38 HV and at HAZ for AS is 36.3 HV – 38.5 HV plus at BM of AS is 45.9 HV to 46.8 HV. TMAZ of AS side appeared to be the softest region for one pass. The highest hardness region exhibited by base metal at both AS and RS side.

Table 4.3: Indentation at each zone for Two Pass

<ul style="list-style-type: none">• Base Metal, RS	
<ul style="list-style-type: none">• Heat Affected Zone, RS	

<ul style="list-style-type: none"> • Thermo-mechanically Affected Zone, RS 	
<ul style="list-style-type: none"> • Weld Zone 	
<ul style="list-style-type: none"> • Thermo-mechanically Affected Zone, AS 	
<ul style="list-style-type: none"> • Heat Affected Zone, AS 	
<ul style="list-style-type: none"> • Base Metal, AS 	

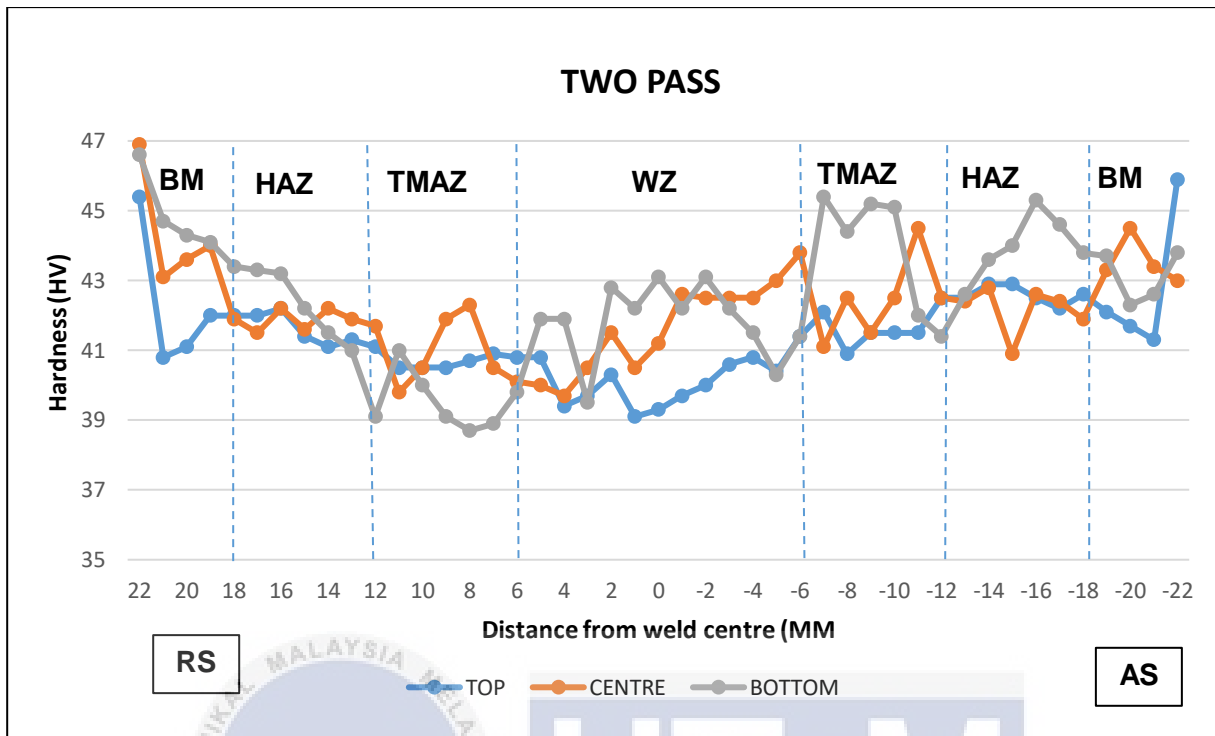


Figure 4.3: Microhardness graph for two pass

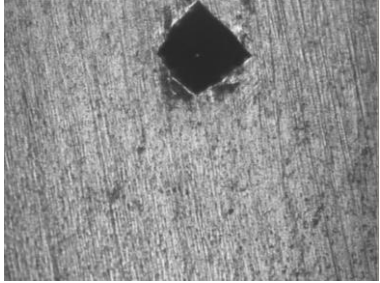
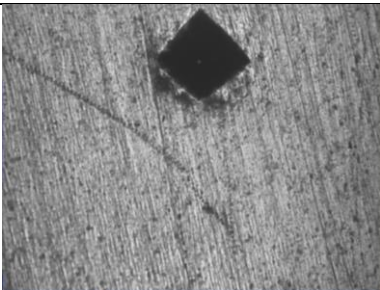
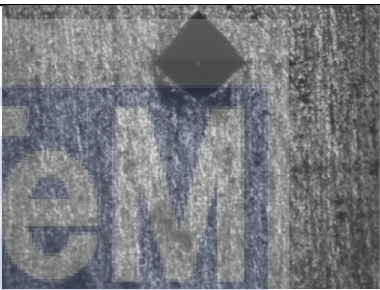
Figure 4.2 presents the microhardness profile of two pass by BFSW process on sample. The initial hardness value for top, centre and bottom is 45.4 HV, 46.9 HV and 46.6 HV. The value of hardness decreases at region of 16 mm to 15 mm from centre of weld. Value of hardness at region from 16 mm to 15 mm for top part declined from 42.2 HV to 41.4 HV for about 1.9% and for centre part decreases about 42.2 HV to 41.6 HV with percentage drop of 1.4%. As for bottom part, hardness reduced from 43.2 HV to 36.5 HV for about 15%. At region -18 mm to -19 mm, hardness value decrease for top part from 42.6 HV to 42.1 HV for about 1.17% and for centre part is increased from 41.9 HV to 43.3 HV with percentage of 3.34%. Meanwhile, hardness value declined from 43.8 HV to 43.7 HV for about 0.22%. Magnitude of hardness is higher in two pass in contrast with one pass.

For two pass, hardness range for base metal (BM) of retreating side (RS) is 40.8 HV – 46.6 HV and for heat affected zone (HAZ) of RS is 41 HV – 43.3 HV. Zone known as thermo-mechanically affected zone (TMAZ) at RS exhibit hardness range of 38.7 HV – 42.3 HV and for weld zone (WZ) is 39.1 HV – 43.1 HV. Moreover, hardness range at TMAZ for advancing side (AS) is 40.9 HV – 45.4 HV and at HAZ for AS is 40.9 HV – 45.3 H. In addition, hardness range at BM of AS is 41.3 HV – 45.9 HV. The softest region at two pass is TMAZ at RS side

and base metal at both RS and AS side are the hardest regions.

Table 4.4: Indentation at each zone for Three Pass

<ul style="list-style-type: none">• Base Metal, RS	
<ul style="list-style-type: none">• Heat Affected Zone, RS	
<ul style="list-style-type: none">• Thermo-mechanically Affected Zone, RS	
<ul style="list-style-type: none">• Weld Zone	

<ul style="list-style-type: none"> • Thermo-mechanically Affected Zone, AS 	
<ul style="list-style-type: none"> • Heat Affected Zone, RS 	
<ul style="list-style-type: none"> • Base Metal, RS 	

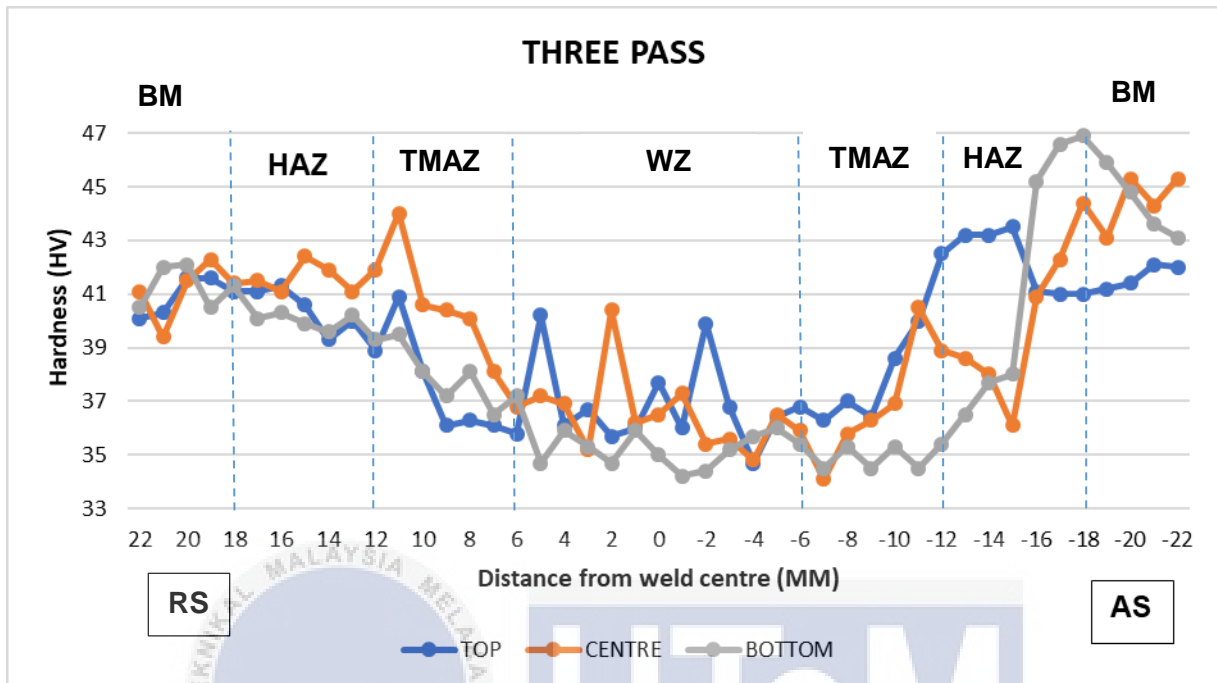


Figure 4.4: Microhardness graph for three pass

Figure 4.3 shows hardness result of three pass welded by BFSW. Starting magnitude of RS for the sample is 45.4 HV for top, 46.9 HV for centre and 46.4 HV for bottom. At region from 16 mm to 15 mm, hardness at top reduced from 41.3 HV to 40.6 HV with percentage about 1.69% and hardness increase from 41.1 HV to 42.4 HV for centre about 3.16%. Furthermore, hardness value at bottom of the sample reduced from 40.3 HV to 39.9 HV with percentage of 0.99%. At region -18 mm to -19 mm, hardness magnitude at top inclined from 41 HV to 41.2 HV for about 0.49 %. As for centre part, percentage of hardness is 2.9% as hardness value decrease from 44.4 HV to 43.1 HV. Hardness value at bottom part declined from 46.9 HV to 45.9 HV with percentage about 2.1%. Magnitude of hardness is lower in three pass in contrast with two pass.

For three pass, hardness range for each zone starting from base metal (BM) of retreating side (RS) is 39.4 HV – 42.3 HV and for heat affected zone (HAZ) of RS is 39.6 HV – 42.4 HV. Meanwhile, thermo-mechanically affected zone (TMAZ) at RS shows range of hardness about 36.1 HV – 44 HV. Hardness range at weld zone (WZ) is 34.2 HV – 40.4 HV. Range of hardness

at TMAZ for advancing side (AS) is 34.5 HV – 42.5 HV and for HAZ of AS is 36.1 HV – 46.9 HV and also 41.2 HV – 45.9 HV for AS in BM zone. Weld zone region is the softest part of the sample and hardest part is exhibited by base metal at AS side in three pass. Overall, two pass produced highest value of hardness range at weld zone, heat affected zone and thermo-mechanically zone for AS side when compared with one and three pass.

Based on microhardness test that was carried out, AA1100 that have been welded by two pass of BFSW have the highest hardness when compared with one and three pass. AA1100 welded by two pass possessed higher hardness than one pass as it received sufficient heat energy during welding process. As it required sufficient heat energy, the heat caused the size of grain to be smaller that enhance its mechanical property in term of hardness. This is due to Hall–Petch relationship that states decrease in size of grains enhanced mechanical property of a metal (Li, Bushby, & Dunstan, 2016). Two pass produced further grain recrystallization at weld zone area than single pass. As the average grain size became smaller, the magnitude of hardness increased. AA1100 welded by one pass exhibited lower hardness than double pass as it did not received adequate heat energy for recrystallization of grains.

Furthermore, sample welded by three pass indicated lower magnitude of hardness than double pass. When number of pass increase from one pass to two pass, it resulted increase in hardness however when two pass increased to three pass, it caused decrease in hardness of AA1100. AA1100 exposed to higher heat in three pass than one and two pass. One of elements that gave impact to the declination of hardness at weld zone was the exposure to high heat energy. This is due to that high heat energy resulted from stirring action caused enlargement in grain size. Enlargement of grain size also resulted from slower cooling rate. Thus, additional growth occurred in grains and it lowered hardness properties of weld zone area in three pass.

4.4 ANALYSIS OF ULTIMATE TENSILE TESTING

Table 4.5: Result of ultimate tensile testing for samples

SAMPLE	1 st pass	2 nd pass	3 rd pass
A	75.80 MPa	83.45 MPa	82.75 MPa
B	76.30 MPa	85.55 MPa	81.35 MPa
Average Ultimate Tensile Strength (Mpa)	76.05 MPa	84.50 MPa	82.05 MPa

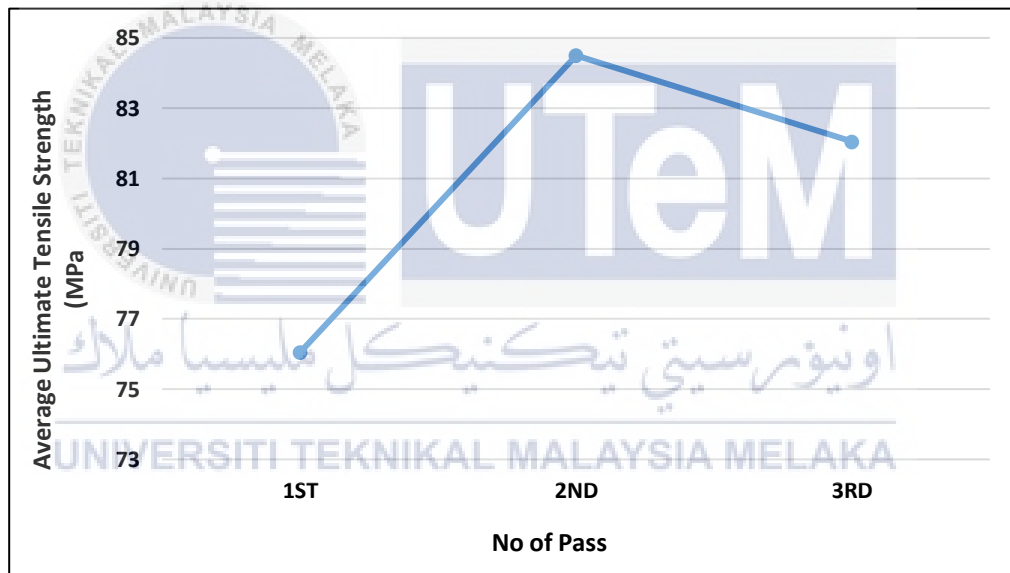


Figure 4.5: Graph of Average Ultimate Tensile Strength (Mpa) vs no of pass

The ultimate tensile strength of base metal for aluminium alloy 1100 is 110 Mpa. From graph above, one pass exhibit the lowest ultimate tensile strength, which is 76.05 Mpa in contrast with two pass and three pass. One pass produced declination in ultimate tensile strength for about 44.6% when compared with base metal. Two pass possessed highest ultimate tensile strength value which is 84.5 Mpa. However, the value of ultimate tensile strength does not exceeded the tensile strength of base metal. Decrease of 30.2% from base metal can be observed for ultimate tensile strength in two pass. As the number of pass increased from two

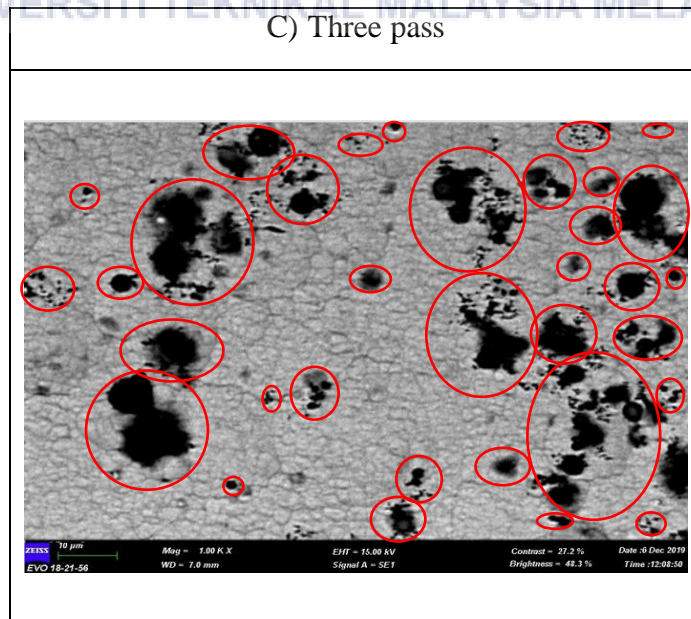
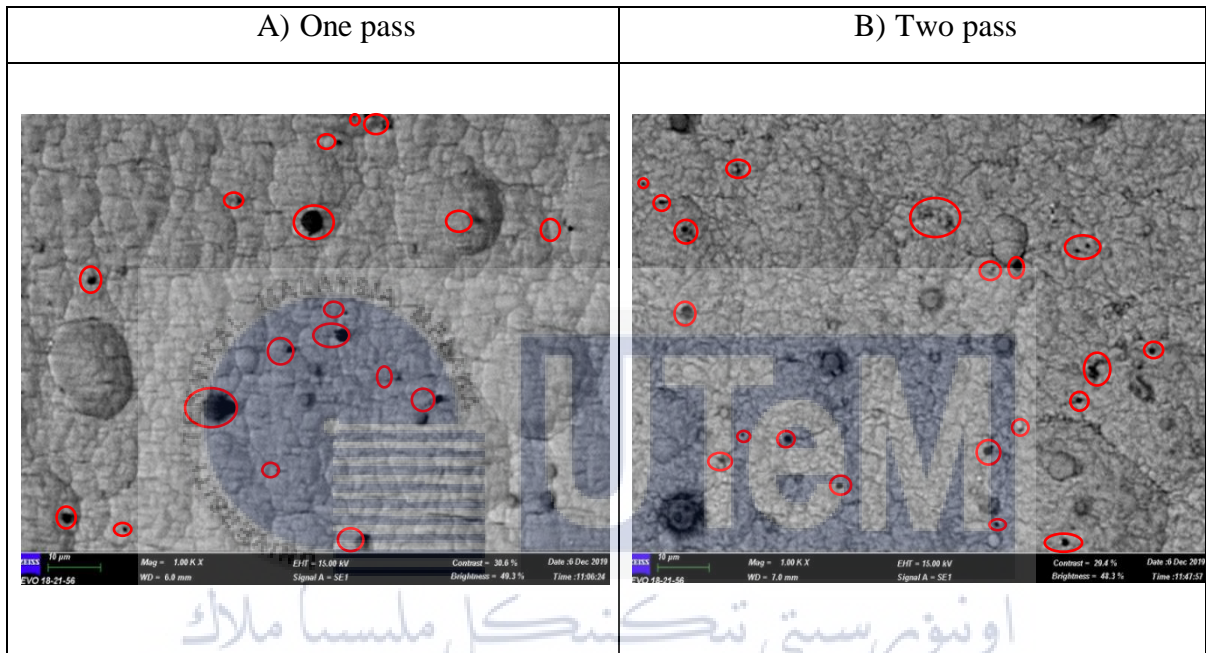
pass to three pass, there is decrease in the ultimate tensile strength about 2.99%. Ultimate Tensile strength for three pass is 82.05 Mpa, which is lower about 34.1% of the the base metal. Overall, two pass produced weld joint that have highest ultimate tensile strength.

A concept that utilized to identify the weld quality is known as joint efficiency. Efficiency of the weld joint can be calculated as ratio ultimate tensile strength of weld joint to the ultimate tensile strength of base metal. Joint efficiency at weld zone for one pass is 69.1% and for two pass is 76.8%. As for three pass, joint efficiency is exhibited as 74.6%. Two pass produced the highest joint efficiency when compared with one pass and three pass. Occurence of further dynamic recrystallization in two pass BFSW enhanced the mechanical property in term of tensile strength. Result of tensile strength is correlated with outcome from microhardness testing.



4.5 MICROSTRUCTURAL OBSERVATION UNDER SCANNING ELECTRON MICROSCOPE

Table 4.6: SEM image at weld zone area for A) one pass, B) two pass and C) three pass magnification of 1000X.



Based on the SEM above, there is occurrence of defect at weld zone area for one pass, two pass and three pass. Type of defect that occurred for each pass is known as porosity. According (Zhang, Lin, Wu, Feng, & Ma, 2006), dark black spot that present on SEM images above known as pores. Black marks that known as pores indicated by red circle. Previous study states that formation of pores caused by oxidation and high speed of welding as pores cannot be filled fully during stirring process. The size of pores is the biggest in three pass joint when compared with one pass joint and two pass joint. Two pass joint has the smallest pores size in contrast with one pass and three pass.

It is believed that absence of shielding gas and the improper welding parameter such as high travel speed of bobbin tool caused the occurrence of pores in the samples. Both of this factor gave a huge impact to weld quality. As for suggestion, the multipass of BFSW should be carried out under presence of shielding gas and at constant travel speed of bobbin tool for each number of pass.

4.6 RESULT FROM FLUID SATURATION LEVEL TEST

Table 4.7: Results from fluid saturation level test

No of pass	Initial mass (g)	Test 1	Test 2	Test 3	Average mass (g)	Difference in mass /density of water (0.99987g/ cm ³)	Percentage of contribution (%)
One pass	8.000	8.020	8.027	8.022	8.023	0.023	2.3
Two pass	9.000	9.000	9.000	9.010	9.003	0.003	0.3
Three pass	9.000	9.031	9.033	9.030	9.031	0.031	3.1

There is presence of pores in one pass, two pass and three pass. Fluid saturation method is used to analyze the level of porosity contribution for the samples. As from table above, porosity level in three pass is the highest compared with one pass and two pass. The porosity level is the lowest in double pass in contrast with one pass and three pass.

CHAPTER 5

CONCLUSION AND RECOMMENDATION

Aluminium alloy 1100 with thickness of 6mm was joined by multipass of bobbin friction stir welding. The hardness and microstructure of sample for one pass, two pass and three pass were analyzed successfully. As from microstructure analysis by optical microscope, shape of grain for one pass, two pass and three pass were able to be examined. Two pass produced weld joint that has fine equiaxed grain structure compared to one pass and three pass. ImageJ software used to calculate the average grain size. Average grain size for one pass is 3.87 μm and for two pass is 2.54 μm . Three pass showed average grain size for about 3.22 μm . When number of pass increased from one pass to two pass, there is declination in average grain size. For three pass, average grain size became higher. Amount of heat input and cooling rate plays vital role in determining grain size.

Based on microhardness test, double pass produced highest hardness when compared with one pass and three pass. The hardness range at weld zone area for two pass is (39.1 HV – 43.1 HV) is the highest among one pass and three pass. Single pass exhibits the lowest hardness value range, which is (34.4 HV – 39.4 HV) in contrast with two pass and three pass. As the number of pass increase from one pass to two pass, hardness is increased. However, when number of pass increase from two pass to three pass, hardness of sample deteriorated which shows hardness range declined to (34.2 HV – 40.4 HV). The hardness property of sample AA 1100 is correlated with the average grain size as it determines the mechanical property. Overall, two pass has the highest tensile strength of 84.05 MPa in contrast with one pass and three pass. It is believed that dynamic recrystallization of grain enhanced the mechanical properties of sample AA1100 in double pass due to adequate input of heat energy from continues stirring action.

According to image from scanning electron microscope, there is presence of defect known as pores in one pass, two pass and three pass. As from fluid saturation level test, porosity level is the highest in three pass and lowest in two pass.

5.1 SUSTAINABILITY

Bobbin friction stir welding process is a good joining process as it does not release any dangerous fumes or gases that threaten the health of human being and safety of environment unlike conventional welding process such as Gas Metal Arc Welding (GMAW) and Shielded Metal Arc Welding (SMAW). Furthermore, it does not produce any harmful ultraviolet ray or radiation. In addition, BFSW is more convenient when compared with fusion welding as it does not require presence of filler material for joining.

In BFSW, usage of bobbin tool reduces the disposal waste rate of filler material. Therefore, it considered as a sustainable process of joining. Consequently, welder can reduce cost on supply of filler material by utilizing BFSW process. Not to mention, Bobbin stir friction welding (BSFW) is an effective welding method as it uses less energy for joining. Thus, it has high demand in manufacturing industry such as automotive industry

5.2 RECOMMENDATION

Although this research worked well, there are few issues that need to be given further recommendation for this project. The proposed suggestions are mainly to elevate quality of weld at joint area. The recommendations for this project are:

- i. The multipass BFSW process should be conducted with same speed of traverse and constant speed of bobbin tool rotation.
- ii. Multipass BFSW should be performed with presence of shielding gas and rapid cooling method to avoid any chance for presence of defects.
- iii. Perform microstructural observation under SEM that equipped with Electron Backscattered Diffraction (EBSD) to get grain orientation mapping.
- iv. Perform observation for the welded joint by using Tunneling Electron Microscope (TEM) to get the image of microstructure in detailed manner for further analysis.

REFERENCE

- Abd Elnabi, M. M., Elshalakany, A. B., Abdel-Mottaleb, M. M., Osman, T. A., & El Mokadem, A. (2019). Influence of friction stir welding parameters on metallurgical and mechanical properties of dissimilar AA5454–AA7075 aluminum alloys. *Journal of Materials Research and Technology*. <https://doi.org/10.1016/j.jmrt.2018.10.015>
- Avila, J. A., Rodriguez, J., Mei, P. R., & Ramirez, A. J. (2016). Microstructure and fracture toughness of multipass friction stir welded joints of API-5L-X80 steel plates. *Materials Science and Engineering: A*, 673, 257–265. <https://doi.org/10.1016/j.msea.2016.07.045>
- Cetkin, E., Çelik, Y. H., & Temiz, S. (2019). Microstructure and mechanical properties of AA7075/AA5182 jointed by FSW. *Journal of Materials Processing Technology*, 268, 107–116. <https://doi.org/10.1016/j.jmatprotec.2019.01.005>
- Derazkola, H. A., Aval, H. J., & Elyasi, M. (2015). Analysis of process parameters effects on dissimilar friction stir welding of AA1100 and A441 AISI steel. *Science and Technology of Welding and Joining*, 20(7), 553–562. <https://doi.org/10.1179/1362171815Y.0000000038>
- Devaiah, D., Kishore, K., & Laxminarayana, P. (2018). Optimal FSW process parameters for dissimilar aluminium alloys (AA5083 and AA6061) Using Taguchi Technique. *Materials Today: Proceedings*, 5(2), 4607–4614. <https://doi.org/10.1016/j.matpr.2017.12.031>
- Dialami, N., Cervera, M., Chiumenti, M., & Segatori, A. (2019). Prediction of joint line remnant defect in friction stir welding. *International Journal of Mechanical Sciences*, 151, 61–69. <https://doi.org/10.1016/j.ijmecsci.2018.11.012>

- Elcoate, C. D., Dennis, R. J., Bouchard, P. J., & Smith, M. C. (2005). Three dimensional multi-pass repair weld simulations. *International Journal of Pressure Vessels and Piping*, 82(4), 244–257. <https://doi.org/10.1016/j.ijpvp.2004.08.003>
- Fuse, K., & Badheka, V. (2019). Bobbin tool friction stir welding: a review. *Science and Technology of Welding and Joining*, 24(4), 277–304. <https://doi.org/10.1080/13621718.2018.1553655>
- Ganesh, K. C., Balasubramanian, K. R., Vasudevan, M., Vasantharaja, P., & Chandrasekhar, N. (2016). Effect of Multipass TIG and Activated TIG Welding Process on the Thermo-Mechanical Behavior of 316LN Stainless Steel Weld Joints. *Metallurgical and Materials Transactions B*, 47(2), 1347–1362. <https://doi.org/10.1007/s11663-016-0600-6>
- Huang, R., Ji, S., Meng, X., & Li, Z. (2018). Drilling-filling friction stir repairing of AZ31B magnesium alloy. *Journal of Materials Processing Technology*, 255, 765–772. <https://doi.org/10.1016/j.jmatprotec.2018.01.019>
- Kar, A., Suwas, S., & Kailas, S. V. (2018). Two-pass friction stir welding of aluminum alloy to titanium alloy: A simultaneous improvement in mechanical properties. *Materials Science and Engineering: A*, 733, 199–210. <https://doi.org/10.1016/j.msea.2018.07.057>
- Khan, N. Z., Khan, Z. A., Siddiquee, A. N., Al-Ahmari, A. M., & Abidi, M. H. (2017). Analysis of defects in clean fabrication process of friction stir welding. *Transactions of Nonferrous Metals Society of China*, 27(7), 1507–1516. [https://doi.org/10.1016/S1003-6326\(17\)60171-7](https://doi.org/10.1016/S1003-6326(17)60171-7)
- Khan, N. Z., Siddiquee, A. N., Khan, Z. A., & Shihab, S. K. (2015). Investigations on tunneling and kissing bond defects in FSW joints for dissimilar aluminum alloys. *Journal of Alloys and Compounds*, 648, 360–367. <https://doi.org/10.1016/j.jallcom.2015.06.246>

- Kulkarni, B. S., Pankade, S. B., Andhale, S. R., & Gogte, C. L. (2018). Effect of backing plate material diffusivity on microstructure, mechanical properties of friction stir welded joints: A Review. *Procedia Manufacturing*, 20, 59–64. <https://doi.org/10.1016/j.promfg.2018.02.008>
- Lambiase, F., Paoletti, A., Grossi, V., & Di Ilio, A. (2019). Analysis of loads, temperatures and welds morphology in FSW of polycarbonate. *Journal of Materials Processing Technology*, 266, 639–650. <https://doi.org/10.1016/j.jmatprotec.2018.11.043>
- Leitao, C., Arruti, E., Aldanondo, E., & Rodrigues, D. M. (2016). Aluminium-steel lap joining by multipass friction stir welding. *Materials & Design*, 106, 153–160. <https://doi.org/10.1016/j.matdes.2016.05.101>
- Liu, H., & Zhang, H. (2009). Repair welding process of friction stir welding groove defect. *Transactions of Nonferrous Metals Society of China*, 19(3), 563–567. [https://doi.org/10.1016/S1003-6326\(08\)60313-1](https://doi.org/10.1016/S1003-6326(08)60313-1)
- Liu, Z. Y., Xiao, B. L., Wang, W. G., & Ma, Z. Y. (2013). Developing high-performance aluminum matrix composites with directionally aligned carbon nanotubes by combining friction stir processing and subsequent rolling. *Carbon*, 62, 35–42. <https://doi.org/10.1016/j.carbon.2013.05.049>
- López-Ortega, A., Bayón, R., & Arana, J. L. (2018). Evaluation of protective coatings for offshore applications. Corrosion and tribocorrosion behavior in synthetic seawater. *Surface and Coatings Technology*, 349, 1083–1097. <https://doi.org/10.1016/j.surfcoat.2018.06.089>
- Muthu Krishnan, M., Maniraj, J., Deepak, R., & Anganan, K. (2018). Prediction of optimum welding parameters for FSW of aluminium alloys AA6063 and A319 using RSM and ANN. *Materials Today: Proceedings*, 5(1), 716–723.

<https://doi.org/10.1016/j.matpr.2017.11.138>

Padhy, G. K., Wu, C. S., & Gao, S. (2018). Friction stir based welding and processing technologies - processes, parameters, microstructures and applications: A review. *Journal of Materials Science & Technology*, 34(1), 1–38.

<https://doi.org/10.1016/j.jmst.2017.11.029>

Salami, P., Khandani, T., Asadi, P., & Besharati Givi, M. K. (2014). Friction stir welding/processing as a repair welding. In *Advances in Friction-Stir Welding and Processing* (pp. 427–457). <https://doi.org/10.1533/9780857094551.427>

Shanavas, S., & Raja Dhas, J. E. (2017). Weldability of AA 5052 H32 aluminium alloy by TIG welding and FSW process – A comparative study. *IOP Conference Series: Materials Science and Engineering*, 247, 012016. <https://doi.org/10.1088/1757-899X/247/1/012016>

Shashi Kumar, S., Murugan, N., & Ramachandran, K. K. (2019). Identifying the optimal FSW process parameters for maximizing the tensile strength of friction stir welded AISI 316L butt joints. *Measurement*, 137, 257–271. <https://doi.org/10.1016/j.measurement.2019.01.023>

Singh, R., Singh, I., Sandhu, G. S., Khan, F., & Singh, J. (n.d.). Mechanical and Metallurgical Properties of Multipass Friction Stir Welded Joints of Aluminium 6061 Alloy. *International Journal of Advance Engineering and Research Development*, 4(4), 10.

Sued, M K, Samsuri, S. S. M., Kassim, M. K. A. M., & Nasir, S. N. N. M. (2018). Sustainability of Welding Process through Bobbin Friction Stir Welding. *IOP Conference Series: Materials Science and Engineering*, 318, 012068. <https://doi.org/10.1088/1757-899X/318/1/012068>

Sued, Mohammad K., & Pons, D. J. (2016). Dynamic Interaction between Machine, Tool, and

- Substrate in Bobbin Friction Stir Welding. *International Journal of Manufacturing Engineering*, 2016, 1–14. <https://doi.org/10.1155/2016/8697453>
- Verma, J., Taiwade, R. V., Reddy, C., & Khatirkar, R. K. (2018). Effect of friction stir welding process parameters on Mg-AZ31B/Al-AA6061 joints. *Materials and Manufacturing Processes*, 33(3), 308–314. <https://doi.org/10.1080/10426914.2017.1291957>
- Vural, M. (2014). Welding Processes and Technologies. In *Comprehensive Materials Processing* (pp. 3–48). <https://doi.org/10.1016/B978-0-08-096532-1.00603-8>
- Węglowski, M. S. (2018). Friction stir processing – State of the art. *Archives of Civil and Mechanical Engineering*, 18(1), 114–129. <https://doi.org/10.1016/j.acme.2017.06.002>
- Xu, N., Ueji, R., & Fujii, H. (2015). Enhanced mechanical properties of 70/30 brass joint by multi-pass friction stir welding with rapid cooling. *Science and Technology of Welding and Joining*, 20(2), 91–99. <https://doi.org/10.1179/1362171814Y.0000000261>
- Yazdipour, A., & Heidarzadeh, A. (2016). Effect of friction stir welding on microstructure and mechanical properties of dissimilar Al 5083-H321 and 316L stainless steel alloy joints. *Journal of Alloys and Compounds*, 680, 595–603. <https://doi.org/10.1016/j.jallcom.2016.03.307>
- Zeinoddini, M., Arnavaz, S., Zandi, A. P., & Vaghasloo, Y. A. (2013). Repair welding influence on offshore pipelines residual stress fields: An experimental study. *Journal of Constructional Steel Research*, 86, 31–41. <https://doi.org/10.1016/j.jcsr.2013.03.010>
- Li, Y., Bushby, A. J., & Dunstan, D. J. (2016). The Hall-Petch effect as a manifestation of the general size effect. *Proceedings of the Royal Society A: Mathematical, Physical and Engineering Sciences*, 472(2190), 1–33. <https://doi.org/10.1098/rspa.2015.0890>

M.K.A.M. Kassim , M.K. Sued and D.J. Pons . (2019). *MECHANICAL PROPERTIES OF THICK AND THIN AA1100 WELDED USING BOBBIN FRICTION STIR WELDING*
M.K.A.M. Kassim 1 , M.K. Sued 1 and D.J. Pons 2.

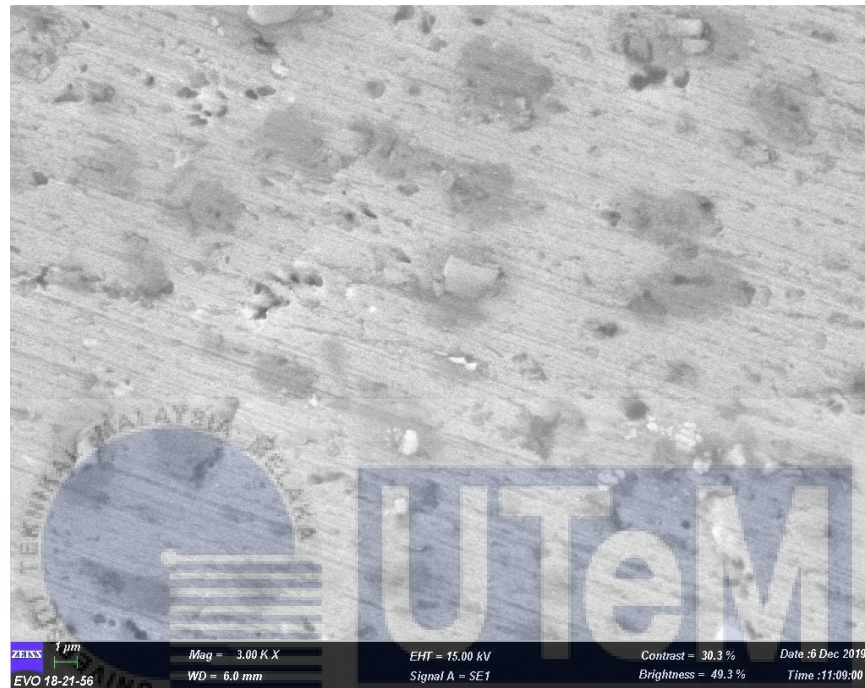
Tamadon, A., Pons, D. J., Sued, K., & Clucas, D. (2018). Formation mechanisms for entry and exit defects in bobbin friction stir welding. *Metals*, 8(1), 1–22.
<https://doi.org/10.3390/met8010033>

Xu, W. F., Luo, Y. X., & Fu, M. W. (2018). Microstructure evolution in the conventional single side and bobbin tool friction stir welding of thick rolled 7085-T7452 aluminum alloy. *Materials Characterization*, 138, 48–55. <https://doi.org/10.1016/j.matchar.2018.01.051>

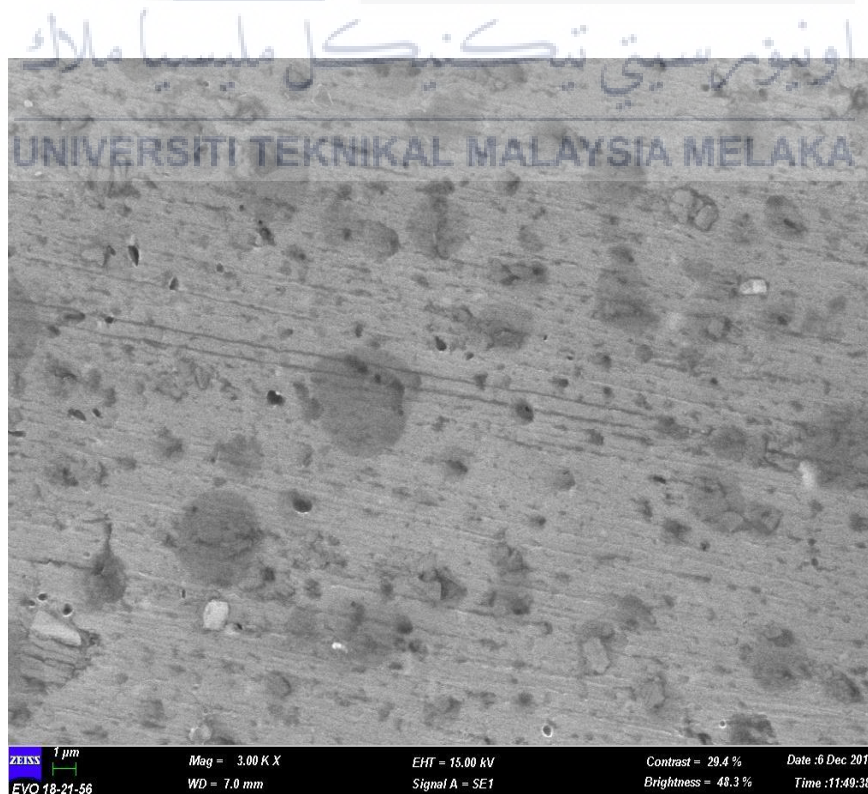
Kowser, M. A., & Motalleb, M. A. (2015). Effect of quenching medium on hardness of carburized low carbon steel for manufacturing of spindle used in spinning mill. *Procedia Engineering*, 105(Icte 2014), 814–820. <https://doi.org/10.1016/j.proeng.2015.05.076>

Zhang, H., Lin, S. B., Wu, L., Feng, J. C., & Ma, S. L. (2006). Defects formation procedure and mathematic model for defect free friction stir welding of magnesium alloy. *Materials and Design*, 27(9), 805–809. <https://doi.org/10.1016/j.matdes.2005.01.016>

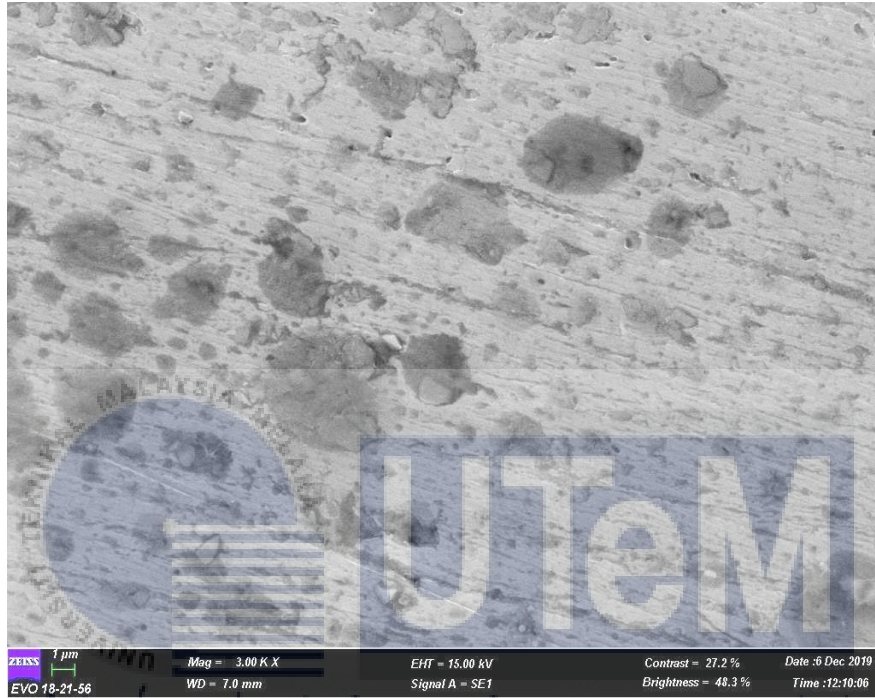
APPENDIX



SEM
image of
One Pass



SEM
image of
Two Pass



SEM
image of
Three
Pass

اونيورسيتي تيكنيكل مليسيا ملاك
UNIVERSITI TEKNIKAL MALAYSIA MELAKA